AD_____

Award Number: W81XWH-07-1-0053

TITLE: Interactions between IGFBP-3 and Nuclear Receptors in Prostate Cancer Apoptosis

PRINCIPAL INVESTIGATOR: Kuk-Wha Lee, M.D.; Ph.D.

CONTRACTING ORGANIZATION: University of California Los Angeles
Los Angeles, CA, 90095

REPORT DATE: January 2008

TYPE OF REPORT: Annual

PREPARED FOR: U.S. Army Medical Research and Materiel Command
Fort Detrick, Maryland 21702-5012

REPORT DOCUMENTATION PAGE

Form Approved
OMB No. 0704-0188

1. REPORT DATE *(DD-MM-YYYY)*	**2. REPORT TYPE**	**3. DATES COVERED** *(From - To)*
01-01-2008	Annual	15 DEC 2006 - 14 DEC 2007

4. TITLE AND SUBTITLE

Interactions Between IGFBP-3 and Nuclear Receptors in Prostate Cancer Apoptosis

5a. CONTRACT NUMBER

5b. GRANT NUMBER
W81XWH-07-1-0053

5c. PROGRAM ELEMENT NUMBER

6. AUTHOR(S)
Kuk-Wha Lee, M.D.; Ph.D.

E-Mail: kukwhalee@mednet.ucla.edu

5d. PROJECT NUMBER

5e. TASK NUMBER

5f. WORK UNIT NUMBER

7. PERFORMING ORGANIZATION NAME(S) AND ADDRESS(ES)

University of California Los Angeles
Los Angeles, CA 90095

8. PERFORMING ORGANIZATION REPORT NUMBER

9. SPONSORING / MONITORING AGENCY NAME(S) AND ADDRESS(ES)
U.S. Army Medical Research and Materiel Command
Fort Detrick, Maryland 21702-5012

10. SPONSOR/MONITOR'S ACRONYM(S)

11. SPONSOR/MONITOR'S REPORT NUMBER(S)

12. DISTRIBUTION / AVAILABILITY STATEMENT
Approved for Public Release; Distribution Unlimited

13. SUPPLEMENTARY NOTES

14. ABSTRACT
IGFBP-3 is a potent inducer of apoptosis in both androgen-dependent and androgen-independent prostate cancer lines. When the nuclear receptor RXRalpha was described as an unexpected intracellular binding partner for IGFBP-3 and effects on DNA transcription were demonstrated, rapid effects of IGFBP-3 on programmed cell death (apoptosis) still could not be explained. These rapid effects on apoptosis were clarified when I hypothesized that IGFBP-3 was a biological signal for Nur77 nuclear receptor translocation to the mitochondria where an apoptotic cascade is initiated. We proposed to determine scientifically the protein regions in each of these important cell death molecules that essential for apoptotic action and demonstrate this observation with mouse models. Our data so far reveal a nuclear export sequence in IGFBP-3. Mutation of this sequence impairs its apoptotic activity. Utilizing the IGFBP-3 KO mouse, we show that IGFBP-3's critical role in castration-induced apoptosis. Mating studies are underway to determine the effects of genetically deleting Nur77 and IGFBP-3 in the ontogeny of prostate cancer.

15. SUBJECT TERMS
IGFBP-3, apoptosis, prostate cancer, nuclear receptors

16. SECURITY CLASSIFICATION OF:			**17. LIMITATION OF ABSTRACT**	**18. NUMBER OF PAGES**	**19a. NAME OF RESPONSIBLE PERSON**
a. REPORT	**b. ABSTRACT**	**c. THIS PAGE**			USAMRMC
U	U	U	UU	36	**19b. TELEPHONE NUMBER** *(include area code)*

Table of Contents

Introduction

Prostate Cancer (CaP) continues to be the most frequently occurring malignancy (aside from skin cancers), found in American men. IGFBP-3 is a potent inducer of apoptosis in both androgen-dependent and androgen-independent prostate cancer lines. When the nuclear receptor RXRalpha was described as an unexpected intracellular binding partner for IGFBP-3 and effects on DNA transcription were demonstrated, rapid effects of IGFBP-3 on programmed cell death (apoptosis) still could not be explained. These rapid effects on apoptosis were clarified when I hypothesized that IGFBP-3 was a biological signal for Nur77 nuclear receptor translocation to the mitochondria where an apoptotic cascade is initiated. This project will determine scientifically the protein regions in each of these important cell death molecules that essential for apoptotic action and demonstrate this observation with mouse models. The innovative aspects of this grant include: (1) Characterization of a novel interface (i.e. mitochondrial localization) of nuclear receptor / IGFBP superfamilies in the initiation of tumor programmed cell death; (2) Development of pre-clinical mouse models of prostate cancer that can be used to assess therapies that exploit the IGFBP-3:Nur77:RXR cell death pathway; and (3) provide a compelling rationale for Phase I studies of IGFBP-3 (or small molecule mimetics of this pathway) in men with prostate cancer.

Body

Task 1. Characterize IGFBP-3 protein-protein interactions and mitochondrial targeting in vitro and demonstrate that they are essential for IGFBP-3 induced apoptosis.

a. Confirm IGFBP-3/RXR/Nur77 ternary complex formation via protein-protein interaction studies. (Months 1-6)

We have established association as published in our *Carcinogenesis* paper (**appendix #1**). We investigated the ability of IGFBP-3 to associate with Nur77 in nuclear and cytoplasmic compartments utilizing co-immunoprecipitation techniques. 22RV1 prostate cancer cells were incubated with 1 mcg/ml of recombinant IGFBP-3 for 2 hours and nuclear and cytoplasmic fractions were isolated as indicated. Protein A-agarose was used to immunoprecipitate bound complexes and these were resolved by SDS-PAGE.

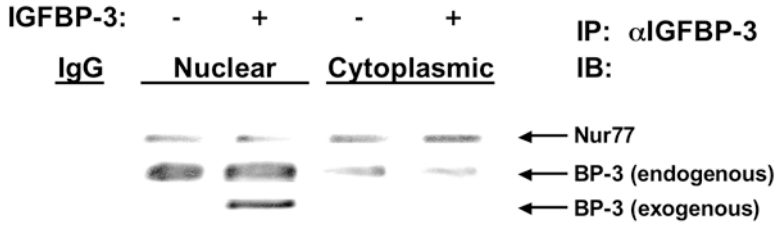

Fig. 1. Interaction between IGFBP-3 and Nur77. 22RV1 cells were incubated with 1 mcg/ml of recombinant IGFBP-3 for 2 hours. Nuclear and Cytoplasmic fractions were isolated as indicated. Protein A-agarose was used to immunoprecipitate bound complexes and resolved by SDS-PAGE. Nur77 and IGFBP-3 were detected by immunoblotting.

Western immunoblotting (Fig. 1) showed that endogenous IGFBP-3 associates with Nur77 in both nuclear and cytoplasmic fractions that is largely unchanged by the addition of exogenous IGFBP-3. Association of Nur77 with control precipitating antibody was not detected. Moreover, detection of IGFBP-3:IGFBP-3 complexes was revealed suggesting that IGFBP-3 can form oligomeric complexes in subcellular compartments. Non-glycosylated IGFBP-3 in this short incubation period was targeted to the nucleus, consistent with our previous observations.

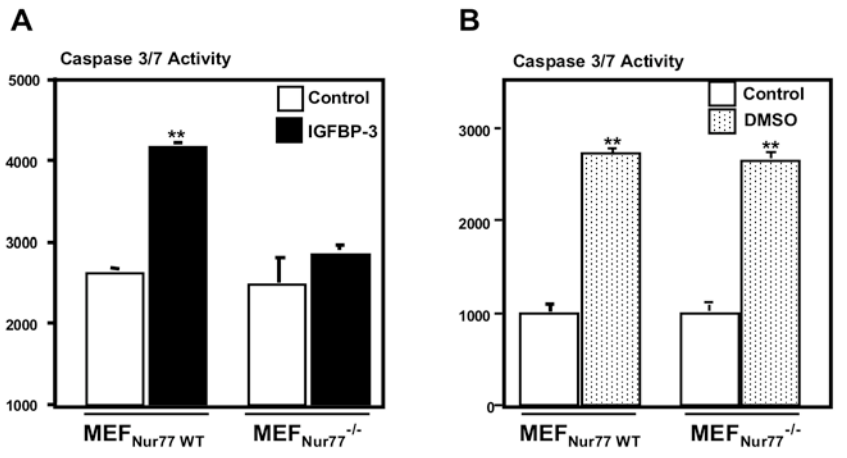

Fig. 2. Nur77 mediates IGFBP-3-induced apoptosis (**A**) Differential response of caspase activation to 2.5 μg/ml IGFBP-3 in Mouse Embryonic Fibroblasts (MEFs) derived from Nur77 Wild-Type (WT) and knockout ($Nur77^{-/-}$) cells. ***P*<0.005 relative to no treatment (Student's t-test). (**B**) Specificity of Nur77 involvement for IGFBP-3 induced apoptosis. Note similar responses to DMSO in WT and knockout line.

To further study the functional interface of IGFBP-3 and Nur77,

we derived Nur77 null (Nur77$^{-/-}$) embryonic fibroblast cells (MEFs) from the Nur77$^{-/-}$ knockout mouse. Using these Nur77 null MEFs, we tested the ability of IGFBP-3 to induce apoptosis (Fig. 2A).

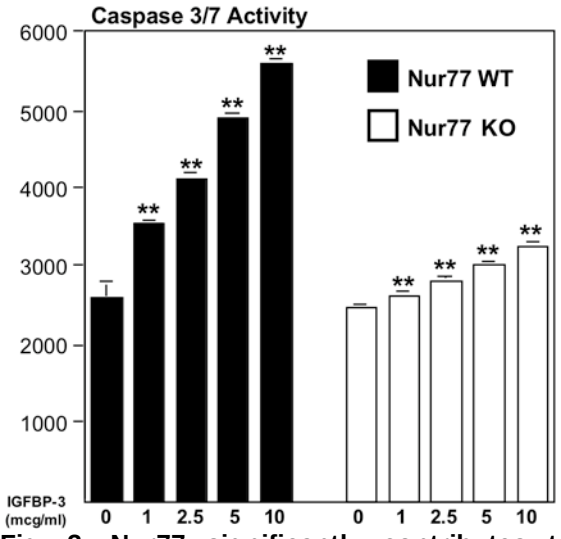

Fig. 3. Nur77 significantly contributes to IGFBP-3 induced apoptosis in a dose-dependent manner. Apoptosis in 22RV1 prostate cancer cells was measured after 48h of transfection by WT and mutant IGFBP-3 in expression vectors by a histone-associated DNA fragment ELISA (Roche).

Overnight treatment with IGFBP-3 resulted in a 60% increase in apoptosis as measured by fluorometric measurement of caspase 3/7 activation in fibroblasts derived from the wild-type animal, but was not able to induce further caspase activation in the line derived from the Nur77$^{-/-}$ knockout animal. The phenomenon was specific to IGFBP-3 induced apoptosis as caspase activation induced by 2% dimethylsulfoxide (DMSO) was not different in WT versus knockout MEFs (Fig. 2B). Thus, Nur77 mediates the pro-apoptotic effect of IGFBP-3.

To more closely examine the role of Nur77 in IGFBP-3 induced apoptosis, we treated Nur77 KO and WT MEFs with increasing doses of recombinant IGFBP-3 that ranged from 1-10 μg/ml over 12 hours (Fig. 3). As expected from the former experiment, IGFBP-3 significantly induced apoptosis in WT MEFs in a dose-dependent manner.

Surprisingly, IGFBP-3 also significantly induced caspase activation in the KO line in a dose-dependent manner, although this was minimal when compared to the WT line. However, this does suggest that a small portion of IGFBP-3 induced caspase activation may be Nur77-independent, although the functional relevance of this is currently unknown.

To validate our findings of Nur77 as a mediator of IGFBP-3 action, we reintroduced Nur77 by transient transfection, with and without co-expression of IGFBP-3. Overexpression of IGFBP-3 alone did not induce caspase activation. Overexpression of Nur77 alone did induce apoptosis activation consistent with previous reports. Reintroduction of Nur77 via transient transfection restored responsiveness to IGFBP-3 overexpression in the Nur77 knockout line (Fig. 4). Thus, rescue of IGFBP-3 induced

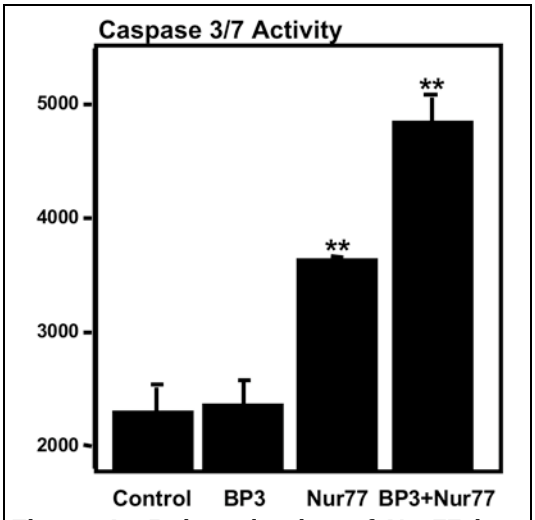

Figure 4. Reintroduction of Nur77 into Nur77 KO MEFs restores responsiveness to IGFBP-3. Values are normalized to b-galactosidase expression to adjust for transfection efficiency. Post 48 hours transfection cells were taken SF overnight and treated for 12 hours with the indicated doses of IGFBP-3 $^{**}P<0.005$ relative to control vector alone, and also for combination compared to Nur77 alone.

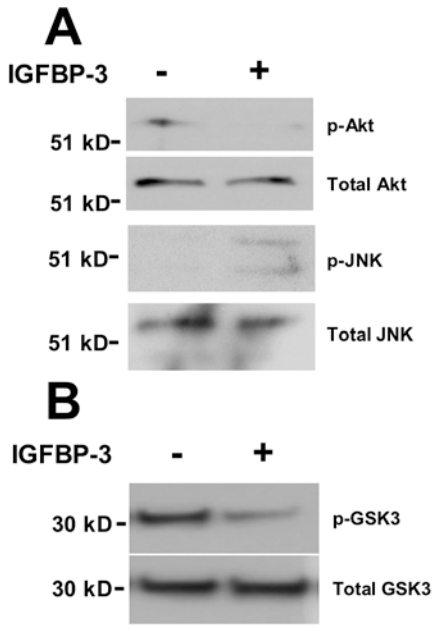

Figure 5. IGFBP-3 induces phosphorylation of c-Jun N-terminal kinase and suppression of Akt phosphorylation and activity.

apoptosis was associated with restoration of Nur77 expression.

Nur77 is phosphorylated by Jun N-terminal kinase (JNK) and by Akt. This phosphorylation is required for its nuclear export and involves JNK activation (phosphorylation) and inhibition of Akt phosphorylation. We investigated the effect of IGFBP-3 treatment of cancer cells on JNK phosphorylation and Akt phosphorylation and activation. (Figure 5) *A*, Western immunoblot for phospho and total Akt; also for phospho and total JNK *B*, Akt kinase assay as assessed by phosphorylation of a GSK-3 fusion protein after immunoprecipitation of Akt. Experiments were repeated three times. Treatment with 1 mcg/ml of IGFBP-3 activated JNK in 22RV1 prostate cancer cells. Associated with this is a significant reduction in phosphorylated Akt and Akt activity as evidence by an Akt kinase assay .

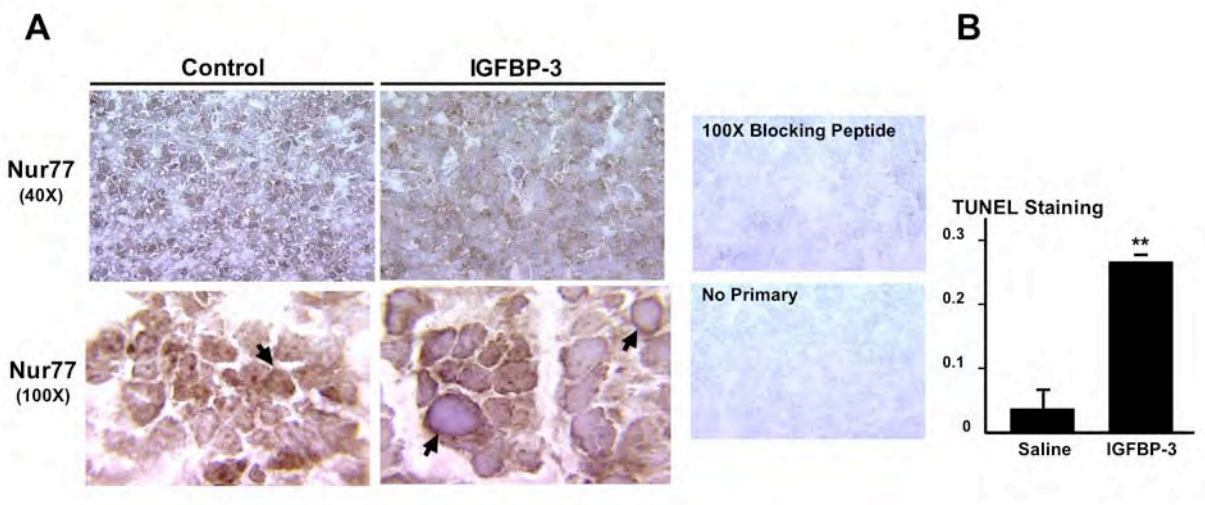

Figure 6. IGFBP-3-induced apoptosis involves translocation of Nur77 in CaP xenografts *in vivo*.. (A) Cross-sectioned LAPC-4 tumors stained with anti- Nur77 (100X, oil immersion). Diaminobenzidine (DAB) was used as a chromogen (dark brown), and commercial hematoxylin was used for counterstaining (blue nuclei). Note predominant nuclear Nur77 staining in control tumor versus empty blue nuclei in the IGFBP-3-treated tumor. Top panel is 40X magnification; lower panel is 100X magnification (oil immersion). Arrows indicate nuclei in which Nur77 is intra-nuclearly stained or translocated to the mitochondria. Control immunohistochemistry shows competition of signal by blocking peptide, as well as lack of binding of secondary antibody. (B) Quantitation of TUNEL staining was used as a measure of apoptosis. TUNEL staining was quantitated by pixel histogram as indicated in bar graph. ***P*<0.005 relative to control treatment.

To determine the effect of IGFBP-3 on Nur77 translocation and apoptosis *in vivo*, we utilized LAPC-4 cells in Matrigel to create human CaP xenografts on SCID mice. Accordingly, cells were injected and tumors established for 2 weeks. At that time, IGFBP-3 or saline was given as a daily injection at a dose of 4 mg/kg/d intraperitoneally (IP) for 21 days, after which mice were euthanized. Tumor sections were stained with a Nur77 antibody to assess subcellular localization in response to IGFBP-3 as well as subjected to TUNEL staining as a marker for apoptosis. Consistent with our *in vitro* data, Nur77 exhibited a predominantly nuclear staining pattern in the rapidly growing control tumors (Fig. 6A, upper panels). Treatment with IGFBP-3 resulted in predominantly cytoplasmic staining of Nur77 with hematoxylin-counterstained nuclei prominent (Fig. 6A, lower panels). Associated with this was a marked significant increase in staining for TUNEL as a marker of apoptosis (Fig. 6B). In concert, these data support a novel extra-nuclear mechanistic role for the orphan receptor Nur77 in mediating the apoptotic actions of IGFBP-3 *in vitro* and *in vivo*.

b. Validate a putative nuclear export sequence (NES) in IGFBP-3. (Months 7-9).
We have successfully created the NES sequence mutants via 2 round PCR, and are characterizing the response to Leptomycin B currently. Primers used were L224A_L227A, 5'-ggaagacacactgaatcac**gc**gaagttc**gc**caatgtgctgagtcccagg-3' and L224A_L227A_antisense 5'-cctgggactcagcacattg**gc**gaactt**cg**cgtgattcagtgtgtcttcc-3'. Sequences have been verified.

c. *Delineate the mitochondrial targeting sequence (MTS) in IGFBP-3.* (Months 7-9).

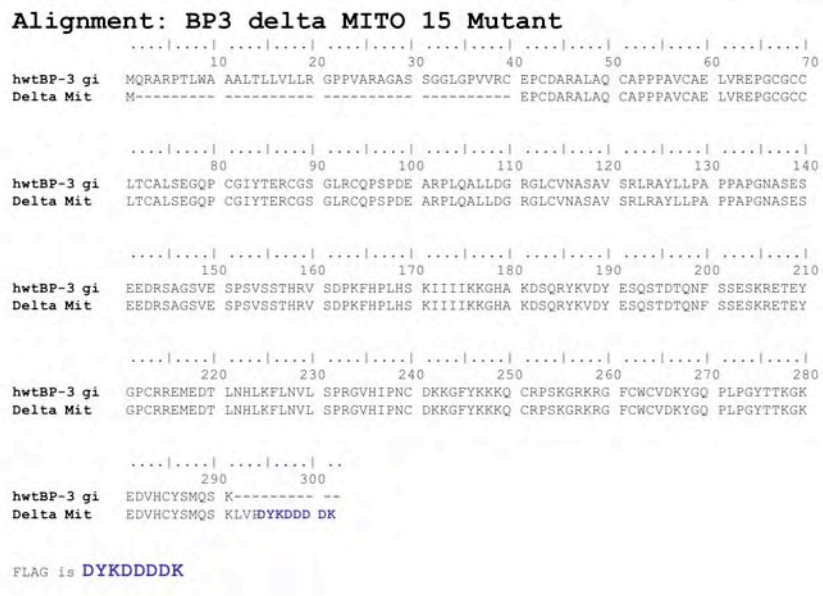

Fig. 7. Verification of the mitochondrial targeting sequence (MTS) mutant by sequencing.

We have constructed the MTS-deletion mutants of IGFBP-3 with FLAG fusions via PCR and are characterizing subcellular co-localization with organelle specific markers currently with various imaging techniques.

d. *Assess the effects of mutant IGFBP-3 (NES and MTS) on apoptosis. (Months 9-12)*

We have begun to assess the effects of the NES and MTS mutants on apoptosis and show that mutation prevents effeicient apoptosis by IGFBP-3. (**Fig. 8**)

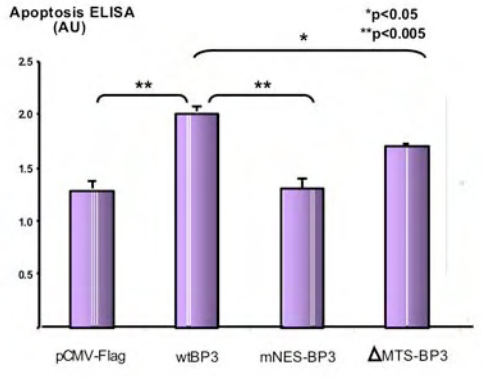

Fig. 8. Mutation of the NES and MTS prevent efficient apoptosis by IGFBP-3. Apoptosis in 22RV1 prostate cancer cells was measured after 48h of transfection by WT and mutant IGFBP-3 by Lipofectamine in expression vectors by a histone-associated DNA fragment ELISA (Roche).

Task 2. Define the role of the IGFBP-3/RXR/Nur77 apoptotic pathway in vivo in the TRAMP mouse model.

a. We will age the Nur77 KO and IGFBP-3 KO mice to determine if and when these mice develop prostatic pre-neoplastic lesions. (Months 1-18)

We have established cohorts and are currently aging them.

b. Examine the role of IGFBP-3 in apoptosis induced by androgen withdrawal by castration of TRAMP and IGFBP-3 KO:TRAMP mice

i. Develop IGFBP-3 KO:TRAMP cross and assess mouse aging and tumor chronomics. (Months 1-24). Total 100 mice.

We are currently breeding these mice and genotyping. After some initial problems with mouse mating (mice were not mating secondary to loud construction noise from adjacent building project), we are happy to report that after moving to a new location the mice have resumed breeding.

ii. Examine subcellular localization of RXR, IGFBP-3, and Nur77 utilizing *in situ* immunohistochemistry and immunoblot post cellular fractionation in tumors before and after castration (25 mice/group; 13 castration and 12 "sham" castration) at 12 weeks of age (Total 75 mice). Animals to be sacrificed after 6h (2 mice/group) and then every 24h for 4 days. (months 1-6)

iii. Evaluate apoptosis utilizing TUNEL staining and evaluate protein subcellular distribution of IGFBP-3, RXR, and Nur77 by Western blotting. (Months 6-12) (**Fig. 9**).

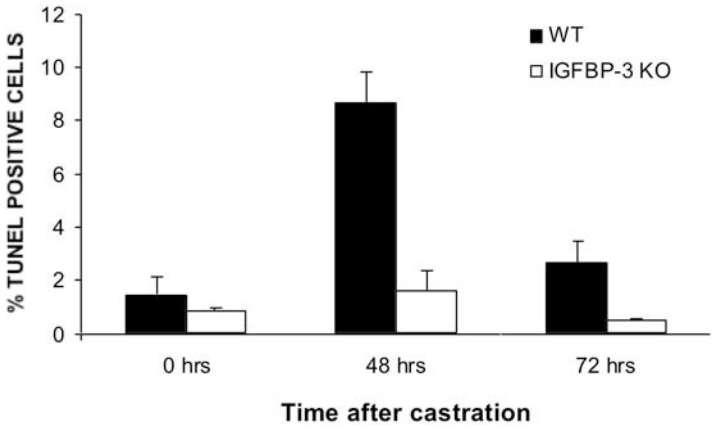

Fig. 9. IGFBP-3 is essential for androgen deprivation induced apoptosis. Twelve-week-old male wild type (WT) mice and IGFBP-3 KO mice were surgically castrated. Prostates were harvested after 48 and 72 hours. Prostates and testes were fixed and stained with H&E for morphologic analysis and quantification of apoptosis using a TUNEL strategy. Apoptosis was quantified by counting the number of TUNEL-positive cells.

WT mice showed a dramatic, 6-fold, increase in the number of TUNEL-positive nuclei at 48 hours post castration. However, IGFBP-3 KO mice prostates failed to show any significant increase in TUNEL staining at 48 hours. By 72 hours TUNEL staining returned to near baseline levels in WT mice and remained near baseline levels in IGFBP-3 KO mice. Serum IGFBP-3 levels were undetectable in the KO mouse and remained unchanged in WT mice post castration. p53 has been shown to be required for prostatic apoptosis, and we have now shown that IGFBP-3, which is activated downstream of p53, is also required for this process. In summary, this is the first description of an *in vivo* role for IGFBP-3 in physiological cell death and indicates that IGFBP-3 is critical for prostatic apoptosis, a fact with potential therapeutic implications in prostate cancer.

c. Study the *in vivo* effects of IGFBP-3 replacement treatment in the IGFBP-3 KO:TRAMP model of prostate cancer. This will commence at a later date after the cross has been established.
   i. Comparison of response to a 4-week course of IGFBP-3 treatment in the TRAMP and TRAMP/IGFBP-3 KO mice on tumor size and histology. (Months 24-30) 7 mice/group total 28 mice (including controls).
   ii. Evaluation of tumor apoptosis by TUNEL staining and proliferation by PCNA staining. (Months 24-30)
   iii. Perform immunohistochemistry for subcellular localization of IGFBP-3, Nur77, and RXR as well as subcellular fractionation and immunoblotting for IGFBP-3, RXR, and Nur77. (Months 30-36)

Key Research Accomplishments

- Confirmed IGFBP-3/RXR/Nur77 ternary complex formation via protein-protein interaction studies.
- Showed Nur77 mediates IGFBP-3 induced apoptosis
- Showed IGFBP-3 induces JNK phosphorylation and suppression of AKT phosphorylation and activity, necessary for Nur77 translocation
- Demonstrated Nur77 translocation by IGFBP-3 *in vivo*
- Created NES / MTS mutants of IGFBP-3
- Assessed Mutant Effects on IGFBP-3 induced apoptosis
- Castrated IGFBP-3 KO and WT mice
- Demonstrated that IGFBP-3 is essential for androgen deprivation-induced apoptosis
- Initiated IGFBP-3 KO : TRAMP mice mating

Reportable Outcomes

1. Liu B, **Lee KW**, Anzo M, Zhang B, Zi X, Tao Y, Shiri L, Pollak M, Lin S, Cohen P. 2007. IGFBP-3 inhibition of prostate cancer progression involves suppression of angiogenesis. 26:1811-9. *Oncogene*. Appendix #3

2. Kim HS, Ali O, Shim M, **Lee KW**, Vuguin P, Muzumdar R, Barzilai N, Cohen P. 2007. Insulin-like Growth Factor Binding Protein-3 induces insulin resistence *in vitro* and *in vivo*. *Pediatric Res*. 61:159-164. Appendix #2

3. **Lee KW**, Ma L, Cobb L, Paharkova-Vatchkova V, Liu B, Milbrandt J, Cohen P. 2007. Contribution of the Orphan Nuclear Receptor Nur77 to the Apoptotic Action of IGFBP-3. *Carcinogenesis* 28:1653-1658. Appendix #1

Conclusions

Thus, we conclude that IGFBP-3 is a potent apoptosis inducer with potential implications in prostate cancer. IGFBP-3 induces apoptosis of both androgen-dependent and –independent CaP in vitro, and this has recently been demonstrated in vivo. On a cell biology level, to my knowledge IGFBP-3 is the only molecule known with an endocrine (serum carrier for IGF), as well as an auto-/paracrine function (that can be IGF-independent) with nuclear and extranuclear functions. Therefore, the proposed work shifts the current thinking of IGFBP biology. We have begun to characterize how subcellular localization of IGFBP-3 effects apoptosis induction. In addition, we have for the first time implicated IGFBP-3 in physiologic apoptosis induced by androgen deprivation utilizing the IGFBP-3 KO mouse. Practically speaking, the mechanistic work proposed therein represents the foundation for a new therapeutic intervention in the treatment of men with prostate cancer. These experiments will provide a research-based rationale for clinical trials of IGFBP-3 and establish a role for such therapy in androgen-dependent and –independent prostate cancer. IGFBP-3 has recently undergone successful phase 1 studies in humans and is about to enter phase 2 studies in cancer patients. If successful, these expected findings will improve our understanding of this emerging prostate cancer therapy and facilitate further clinical development in men with prostate cancer.

References

- Liu B, **Lee KW**, Anzo M, Zhang B, Zi X, Tao Y, Shiri L, Pollak M, Lin S, Cohen P. 2007. IGFBP-3 inhibition of prostate cancer progression involves suppression of angiogenesis. 26:1811-9. *Oncogene*.

- Kim HS, Ali O, Shim M, **Lee KW**, Vuguin P, Muzumdar R, Barzilai N, Cohen P. 2007. Insulin-like Growth Factor Binding Protein-3 induces insulin resistence *in vitro* and *in vivo*. *Pediatric Res*. 61:159-164.

- **Lee KW**, Ma L, Cobb L, Paharkova-Vatchkova V, Liu B, Milbrandt J, Cohen P. 2007. Contribution of the Orphan Nuclear Receptor Nur77 to the Apoptotic Action of IGFBP-3. *Carcinogenesis* 28:1653-1658.

Carcinogenesis vol.28 no.8 pp.1653–1658, 2007
doi:10.1093/carcin/bgm088
Advance Access publication April 13, 2007

Contribution of the orphan nuclear receptor Nur77 to the apoptotic action of IGFBP-3

Kuk-Wha Lee*, Laura J.Cobb, Vladislava Paharkova-Vatchkova, Bingrong Liu, Jeffrey Milbrandt[1] and Pinchas Cohen

Division of Pediatric Endocrinology, Mattel Children's Hospital at University of California at Los Angeles, David Geffen School of Medicine, 10833 Le Conte Avenue, MDCC 22-315, Los Angeles, CA 90095, USA and [1]Department of Pathology and Immunology, Washington University School of Medicine, St Louis, MO 63110, USA

*To whom correspondence should be addressed. Tel: +1 310 825 6244; Fax: +1 310 206 5843;
Email: kukwhalee@mednet.ucla.edu

Tumor suppression by insulin-like growth factor-binding protein-3 (IGFBP-3) has been demonstrated to occur via insulin-like growth factor-dependent and -independent mechanisms *in vitro* and *in vivo*. We have recently described IGFBP-3-induced mitochondrial translocation of the nuclear receptors RXRα/Nur77 in the induction of prostate cancer (CaP) cell apoptosis. Herein, we demonstrate that IGFBP-3 and Nur77 associate in the cytoplasmic compartment in 22RV1 CaP cells. Nur77 is a major component of IGFBP-3-induced apoptosis as shown by utilizing mouse embryonic fibroblasts (MEFs) derived from Nur77 wild-type and knockout (KO) mice. However, dose–response experiments revealed that a small component of IGFBP-3-induced apoptosis is Nur77 independent. Reintroduction of Nur77 into Nur77 KO MEFs restores full responsiveness to IGFBP-3. IGFBP-3 induces phosphorylation of Jun N-terminal kinase and inhibition of Akt phosphorylation and activity, which have been associated with Nur77 translocation. Finally, IGFBP-3 administration to CaP xenografts on SCID mice induced apoptosis and translocated Nur77 out of the nucleus. Taken together, our results verify an important role for the orphan nuclear receptor Nur77 in the apoptotic actions of IGFBP-3.

Introduction

Prostate cancer (CaP) continues to be the most frequently occurring malignancy (aside from skin cancers) in American men. Large epidemiological studies have shown that serum insulin-like growth factor (IGF)-I levels are elevated and insulin-like growth factor-binding protein-3 (IGFBP-3) levels are reduced in patients with CaP, with differences in these serum markers becoming evident 5 years prior to the development of clinical CaP (1). Multiple lines of *in vitro* and clinical evidence point to IGFBP-3 as an anticancer molecule (2). Indeed, *in vivo* demonstration of tumor suppression by IGFBP-3, either administered to cancer xenografts in combination with an RXR ligand (3) or as evidenced by mice transgenic for IGFBP-3 crossed with animal tumor models (4), has been verified by several groups.

We previously reported that IGFBP-3 induces the intrinsic (mitochondria-dependent) pathway of apoptosis by causing the nuclear receptors RXRα/Nur77 to target mitochondria and induce cytoplasmic cytochrome c release, caspase activation and subsequent apoptosis (5). The orphan nuclear receptor Nur77-dependent apoptotic pathway is unique in that mitochondria-targeted Nur77 induces a conformational change in the pro-survival molecule Bcl-2 and converts it to a 'killer' (6), exemplifying a shifting paradigm for transcription factors at the mitochondria (7). Herein, we report the physical interaction of IGFBP-3 and Nur77, the contribution of Nur77 on IGFBP-3-induced apoptosis and demonstrate for the first time that Nur77 translocation by IGFBP-3 occurs in cancer cells *in vivo*.

Abbreviations: CaP, prostate cancer; IGF, insulin-like growth factor; IGFBP-3, insulin-like growth factor-binding protein-3; JNK, Jun N-terminal kinase; KO, knockout; MEF, mouse embryonic fibroblast; SDS–PAGE, sodium dodecyl sulfate–polyacrylamide gel electrophoresis; TBS, Tris-buffered saline; WT, wild type.

Materials and methods

Materials

Insmed (Glen Allen, VA) provided recombinant human IGFBP-3. Commercial antibodies included the following: anti-human IGFBP-3 from DSL (Webster, TX), anti-Nur77 and blocking peptide were from Geneka Biotechnology (Montreal, Canada) and control goat IgG from Santa Cruz Biotechnologies (Santa Cruz, CA). p-Akt, total Akt, p-Jun N-terminal kinase (JNK) and total JNK antibodies as well as Akt kinase assay were from Cell Signaling Technology (Danvers, MA). Sodium dodecyl sulfate–polyacrylamide gel electrophoresis (SDS–PAGE) reagents, Tween and fat-free milk were purchased from Bio-Rad (Hercules, CA). Enhanced chemiluminescence reagents were from Amersham Pharmacia Biotech (Sunnyvale, CA). Full-length IGFBP-3 and Nur77 cDNAs were cloned into pLP-IRESneo mammalian expression vector via pDNR-mediated Creator™ technology (Clontech, Palo Alto, CA). LipofectAMINE and PLUS reagent were from Invitrogen (Carlsbad, CA). All other chemicals were from Sigma–Aldrich (St. Louis, MO).

Cell culture

22RV1 cells were maintained in Dulbecco's modified Eagle's medium containing 10% fetal calf serum (Life Technologies, Carlsbad, CA), 100 units of penicillin/ml and 100 units of streptomycin/ml in a humidified environment with 5% CO_2. CCRF-CEM cells (American Type Culture Collection, Manassas, VA) were maintained in RPMI 1640 medium with 2 mM L-glutamine adjusted to contain 1.5 g/l sodium bicarbonate, 4.5 g/l glucose, 10 mM *N*-2-hydroxyethylpiperazine-*N*′-2-ethanesulfonic acid and 1.0 mM sodium pyruvate, 90%; fetal bovine serum, 10% (Life Technologies), 100 units of penicillin/ml and 100 units of streptomycin/ml in a humidified environment with 5% CO_2 also. LAPC-4 cells (8) were a kind gift of Dr C.Sawyers (University of California, Los Angeles) and cultured in Iscove's modified Dulbecco's medium containing 10% fetal bovine serum, 1% L-glutamine and 1 nM R1181 (NEN Life Science Products, Boston, MA).

Subcellular fractionation procedures

Nu-CLEAR Protein Extraction kit™ was from Sigma–Aldrich. Subcellular fractions were isolated according to the manufacturer's protocol.

Transient transfections

Cells (2×10^4) were seeded in 96-well culture plates. Transfections were done with LipofectAMINE:PLUS reagent as directed by the manufacturer (Invitrogen). Typically, 50 ng of β-galactosidase expression vector (pSV-β-Gal, Promega, Madison, WI) and 50 ng expression vectors, empty or containing IGFBP-3 and/or Nur77 (to equalize total amount of expression vector), were mixed with carrier DNA to give 0.2 μg total DNA per well. After 24–48 h transfection, caspase activity was quantitated and normalized for transfection efficiency to measurements of aliquots of co-transfected β-galactosidase gene activity (β-galactosidase enzyme assay system, Promega).

Co-immunoprecipitation and western immunoblots

22RV1 nuclear or cytoplasmic extracts were immunoprecipitated with or anti-IGFBP-3 antibodies. Briefly, 250 μl of protein A-agarose was incubated overnight at 4°C with 5 μl of anti-human IGFBP-3 antibodies. One hundred and twenty-five microliters of each antibody-treated protein A-agarose were added to 10 μg of protein extract and incubated for 3 h at 4°C with shaking. Immunoprecipitated proteins were pelleted by centrifugation and washed three times with 100 μl of SACI buffer. Sample buffer (200 μl) was added to each sample and vortexed vigorously. Samples were boiled and vortexed again to release protein–antibody complexes from the protein A-agarose. The protein A-agarose was then separated from the immunoprecipitated complexes by centrifugation. The supernatants were saved, and the immunoprecipitated proteins were separated by non-reducing SDS–PAGE (8%) at constant voltage overnight, and then transferred to nitrocellulose for 4 h at 170 mA. The nitrocellulose was immersed in blocking solution [5% non-fat milk/Tris-buffered saline (TBS)] for 45 min, washed with TBS and 0.1% Tween and incubated with primary anti-human Nur77 or anti-human IGFBP-3 antibody (1:4000) for 2 h. After washing off any unbound antibodies, the nitrocellulose was incubated with a secondary antibody (1:10 000) for 1 h. The membrane was

washed four times with TBS, 0.1% Tween and TBS. Bands were visualized using the peroxidase-linked enhanced chemiluminescence detection system (Amersham Pharmacia Biotech). Experiments were repeated three times.

Caspase assays

The caspase assay was done using Apo-ONE™ homogenous caspase-3/-7 assay (Promega) and performed according to the manufacturer's instructions. rhIGFBP-3 was used at final concentrations of 1–10 μg/ml. Two percent dimethylsulfoxide was used as a control in some experiments.

Generation of Nur77$^{-/-}$ and wild-type primary mouse embryo fibroblast lines

Nur77$^{-/-}$ and wild-type (WT) mice on a C57Bl/6 background were maintained on standard chow. Experiments were conducted in accordance with the Animal Research Committee of the University of California, Los Angeles. Fibroblasts were generated from 13.5-day embryos as described previously (9). Cells were maintained in Dulbecco's modified Eagle's medium containing 10% fetal bovine serum, 1% penicillin–streptomycin and 1% L-glutamine. All cells were used before passage 6.

Kinase assay methods

22RV1 CaP cells were incubated for 24 h in serum-free media in the presence or absence of 1 μg/ml recombinant human IGFBP-3. Akt kinase assay was assessed using a non-radioactive Akt kinase assay kit (Cell Signaling Technology) following the manufacturer's instructions. Briefly, Akt was immunoprecipitated from 100 μg cell lysate overnight using an immobilized Akt antibody. Immunoprecipitated protein was then incubated with 1 μg GSK-3 fusion protein in the presence of ATP for 30 min at 30°C. Proteins were separated by SDS–PAGE and analyzed by autoradiography for phospho and total GSK-3.

Tumor xenografts

The LAPC-4 human CaP cell line expresses a WT androgen receptor and secretes prostate-specific antigen. LAPC-4 xenograft tumors were generated by injection of 1×10^6 cells in 200 μl mixed at a 1:1 dilution with Matrigel in the right flank of male SCID mice. Tumors were established for 2 weeks before the start of treatment. Ten SCID mice with LAPC-4 tumors were treated daily with saline or IGFBP-3 (4 mg/kg/day) given by daily intra-peritoneal injections. The mice were euthanized at 21 days. Tumors were harvested, fixed in formaldehyde and embedded in paraffin.

Immunohistochemical staining for Nur77

Paraffin-embedded, 4 μm thick tissue sections of LAPC-4 xenografts were stained for the Nur77 protein. The sections were deparaffinized in a series of xylene baths and then rehydrated using a graded alcohol series. The sections were then immersed in methanol containing 0.3% hydrogen peroxidase for 20 min to block endogenous peroxidase activity and then incubated in 2.5% blocking serum to reduce non-specific binding. Sections were incubated overnight at 4°C with primary anti-Nur77 antibody (1:100). The sections were then processed using standard avidin–biotin immunohistochemistry techniques according to the manufacturer's recommendations (Vector Laboratories, Burlingame, CA). Diaminobenzidine was used as a chromogen and commercial hematoxylin was used for counterstaining.

TUNEL staining

Paraffin-embedded sections were prepared from LAPC-4 tumors harvested on day 21. After deparaffinization of tissue section, apoptotic DNA fragments were labeled by terminal deoxynucleotidyl transferase and detected by anti-digoxigenin antibody conjugated to fluorescein (ApopTag Fluorescein *In Situ* Apoptosis Detection kit, Chemicon, Temecula, CA). Cells were examined at ×20 using an inverted fluorescence microscope (Axiovert 135M, Carl Zeiss, New York, NY). Apoptotic staining was quantified by pixel histogram (Adobe Systems, Mountain View, CA) and confirmed by manual counting ($r = 0.98$).

Statistical analysis

All experiments were repeated at least three times. Means ± SDs are shown. Statistical analyses were performed using analysis of variance utilizing InStat (GraphPad, San Diego, CA). Differences were considered statistically significant when $P < 0.005$, denoted by $**$.

Results

Subcellular association of IGFBP-3 and Nur77

We and others have described the physical interaction between IGFBP-3 and the nuclear receptors RXRα and RARα (10,11). We investigated the ability of IGFBP-3 to associate with Nur77 in nuclear and cytoplasmic compartments utilizing co-immunoprecipitation techniques. 22RV1 CaP cells were taken serum free overnight. Protein A-agarose was used to immunoprecipitate-bound complexes and these were resolved by SDS–PAGE.

Western immunoblotting (Figure 1) showed that endogenous IGFBP-3 associates with Nur77 in cytoplasmic fractions only and complexes were not detected in nuclear fractions. Controls of whole-cell lysate show presence of endogenous Nur77 and IGFBP-3 in the immunoprecipitation input. CCRF-CEM is a T lymphoblastoid cell line (ATCC), and nuclear extract was used as a positive control for Nur77. The major band of endogenous IGFBP-3 was detected in the nucleus, consistent with our previous observations (12). Similarly, Nur77 is typically a nuclear transcription factor. This observation is indicative of distinctive subcellular co-distribution whereby unassociated Nur77 and IGFBP-3 are prevalent in the nucleus, but their complexes are uniquely cytoplasmic.

Contribution of Nur77 to the apoptotic effects of IGFBP-3

To further study the functional interface of IGFBP-3 and Nur77, we derived Nur77 null (Nur77$^{-/-}$) embryonic fibroblast cells (MEFs) from the Nur77$^{-/-}$ knockout (KO) mouse. Using these Nur77 null MEFs, we tested the ability of IGFBP-3 to induce apoptosis (Figure 2A). Overnight treatment with IGFBP-3 resulted in a 60% increase in apoptosis as measured by fluorometric measurement of caspase-3/-7 activation in fibroblasts derived from the WT animal, but was not able to induce further caspase activation in the line derived from the Nur77$^{-/-}$ KO animal. The phenomenon was specific to IGFBP-3-induced apoptosis as caspase activation induced by 2% dimethylsulfoxide was not different in WT versus KO MEFs (Figure 2B). Thus, Nur77 significantly contributes to the pro-apoptotic effect of IGFBP-3 at this dose.

To more closely examine the role of Nur77 in IGFBP-3-induced apoptosis, we treated Nur77 KO and WT MEFs with increasing doses of recombinant IGFBP-3 that ranged from 1 to 10 μg/ml >12 h (Figure 2C). As expected from the former experiment, IGFBP-3 significantly induced apoptosis in WT MEFs in a dose-dependent manner. Surprisingly, IGFBP-3 also significantly induced caspase activation in the KO line in a dose-dependent manner, although this was minimal when compared with the WT line. However, this does suggest that a small portion of IGFBP-3-induced caspase activation may be Nur77 independent, although the functional relevance of this is currently unknown.

Reintroduction of Nur77 in Nur77 KO MEFs restores responsiveness to IGFBP-3

To validate our findings of Nur77 as a mediator of IGFBP-3 action, we reintroduced Nur77 into Nur77 KO MEFs by transient transfection, with and without co-expression of IGFBP-3. Control transfection was with empty expression vectors and was not significantly different from that of transfection with empty Nur77 expression vector and IGFBP-3 over-expression. Over-expression of Nur77 in combination with empty IGFBP-3 expression vector did induce apoptosis activation consistent with previous reports (13,14). Reintroduction of Nur77 via transient transfection restored responsiveness to IGFBP-3

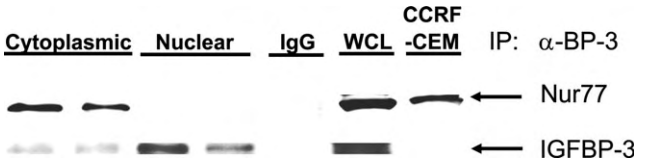

Fig. 1. Cytoplasmic interaction between IGFBP-3 and Nur77. 22RV1 cells were taken serum free overnight and association of endogenous Nur77 and IGFBP-3 was assessed. Nuclear and cytoplasmic fractions were isolated as indicated. Protein A-agarose was used to immunoprecipitate bound complexes and resolved by SDS–PAGE. Nur77 and IGFBP-3 were detected by immunoblotting. 22RV1 whole-cell lysate (WCL) was used as an input control. CCRF-CEM nuclear extract as a positive control for Nur77 presence. Experiments were repeated three times.

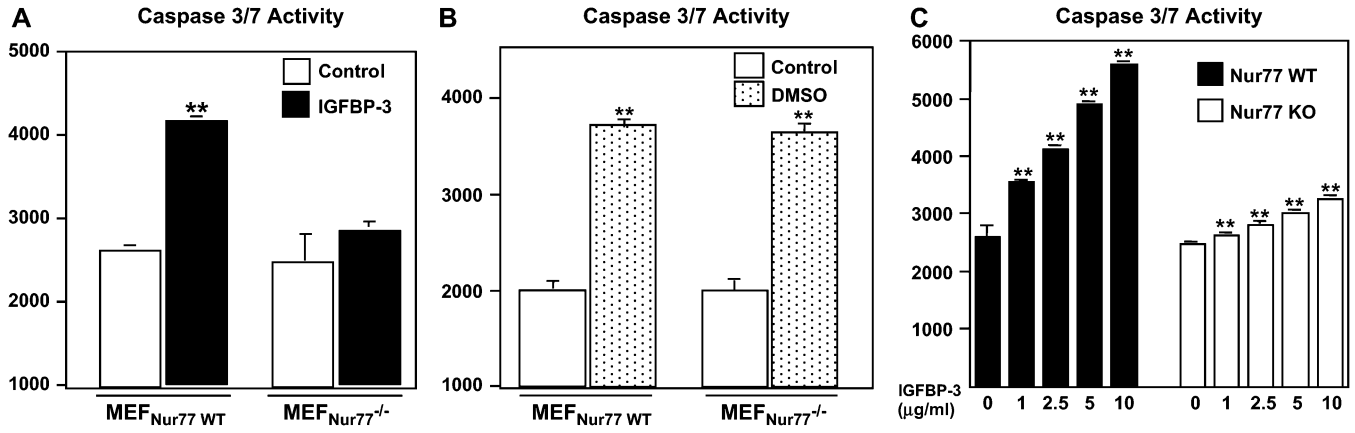

Fig. 2. Nur77 significantly contributes to IGFBP-3-induced apoptosis. (**A**) Differential response of caspase activation to 2.5 μg/ml IGFBP-3 in MEFs derived from Nur77 WT and KO (Nur77$^{-/-}$) cells. $^{**}P < 0.005$ relative to no treatment (Student's *t*-test). (**B**) Specificity of Nur77 involvement for IGFBP-3-induced apoptosis. Note similar responses to dimethylsulfoxide (DMSO) in WT and KO line. (**C**) Nur77 contributes to IGFBP-3-induced apoptosis in a dose-dependent manner. Dose response to indicated concentrations of IGFBP-3 for 12 h. Caspase-3/-7 activity was measured by fluorometric assay. Experiments were repeated three times.

over-expression in the Nur77 KO line (Figure 3). Thus, rescue of IGFBP-3-induced apoptosis was associated with restoration of Nur77 expression.

IGFBP-3 induces phosphorylation of c-JNK and suppression of Akt phosphorylation and activity

Nur77 is phosphorylated by JNK and by Akt (15–17). This phosphorylation is required for its nuclear export and involves JNK activation (phosphorylation) and inhibition of Akt phosphorylation in lung cancer and HEK cells (18). We investigated the effect of IGFBP-3 treatment of cancer cells on JNK phosphorylation and Akt phosphorylation and activation. Treatment with 1 μg/ml of IGFBP-3 for 24 h induced phosphorylation of JNK in 22RV1 CaP cells although the expression levels of total JNK were not changed (Figure 4C). Associated with this is a significant reduction in phosphorylated Akt and Akt activity as evidence by an Akt kinase assay (Figure 4A and B). Thus, the apoptotic action of IGFBP-3, which we have described previously to involved RXR/Nur77 translocation via an IGF-independent mechanism (5), involves inhibition of Akt and phosphorylation of JNK.

IGFBP-3 induces apoptosis and translocates Nur77 in vivo

To determine the effect of IGFBP-3 on Nur77 translocation and apoptosis *in vivo*, we utilized LAPC-4 cells in Matrigel to create human CaP xenografts on SCID mice. Accordingly, cells were injected and tumors established for 2 weeks. At that time, IGFBP-3 or saline was given as a daily injection at a dose of 4 mg/kg/day intra-peritoneally for 21 days, after which mice were euthanized. Tumor sections were stained with a Nur77 antibody to assess subcellular localization in response to IGFBP-3 as well as subjected to TUNEL staining as a marker for apoptosis. Consistent with our *in vitro* data, Nur77 exhibited a predominantly nuclear staining pattern in the rapidly growing control tumors (Figure 5A, upper panels). Treatment with IGFBP-3 resulted in predominantly cytoplasmic staining of Nur77 with hematoxylin-counterstained nuclei prominent (Figure 5A, lower panels). Associated with this was a marked significant increase in staining for TUNEL as a marker of apoptosis (Figure 5B). In concert, these data support a novel extranuclear mechanistic role for the orphan receptor Nur77 in mediating the apoptotic actions of IGFBP-3 *in vitro* and *in vivo*.

Discussion

In the prostate, IGFs and IGFBPs play an important role in the proliferative processes that lead to benign prostatic hyperplasia and CaP.

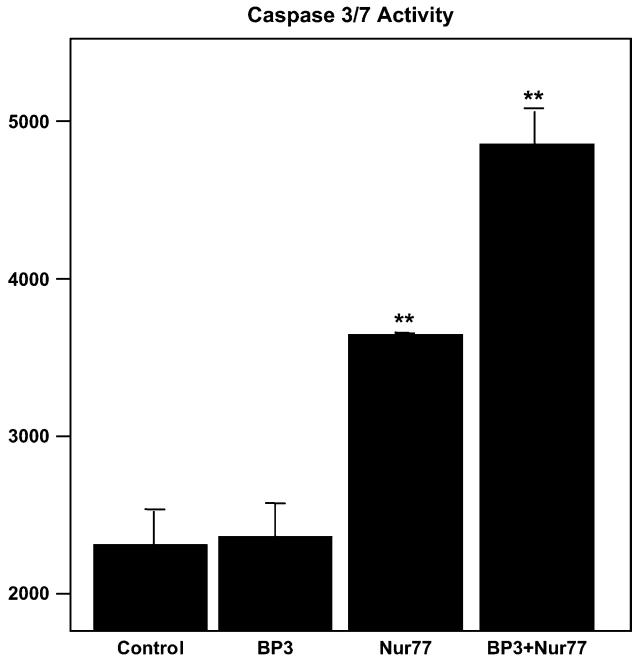

Fig. 3. Reintroduction of Nur77 into Nur77 KO MEFs restores responsiveness to IGFBP-3. Values are normalized to β-galactosidase expression to adjust for transfection efficiency. $^{**}P < 0.005$ relative to control vector alone and also for combination compared with Nur77 alone. Experiments were repeated three times.

IGFBP-3 is secreted and reuptaken by endocytic pathways (specifically caveolin and transferrin receptor mediated) for apoptosis induced by transforming growth factor-β (12). After internalization, IGFBP-3 rapidly localizes to the nucleus where it interacts with RXRα, RAR and potentially RNA Polymerase II binding subunit as recently described (10,11,19), implicating IGFBP-3 as a potential direct modulator of gene transcription. Indeed, IGFBP-3 modulates signaling of nuclear receptor ligands and alters their action (20). Nuclear import of IGFBP-3 is a nuclear localization signal-dependent process and mediated by binding to importin-β (21).

The first *in vivo* validation for IGF-independent actions of IGFBP-3 on tumor suppression has recently been published in a mouse model of CaP (4). Important findings in this study include the

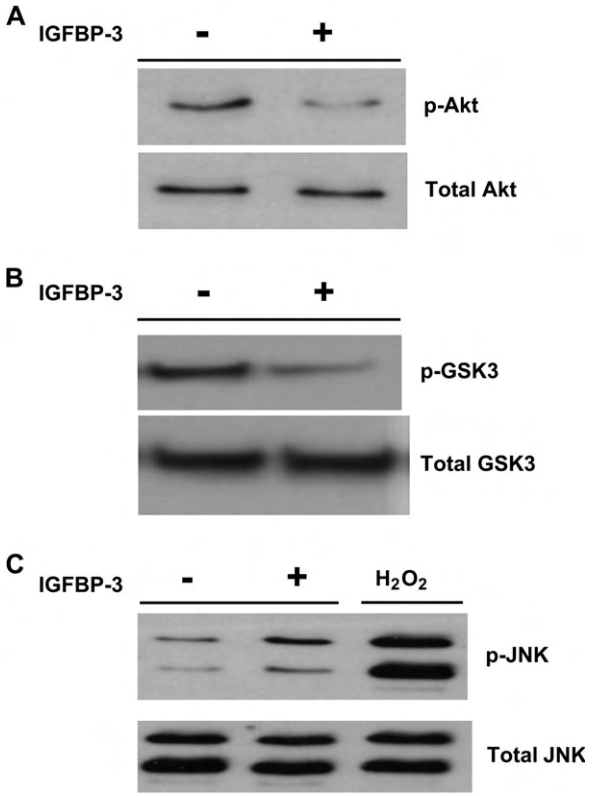

Fig. 4. IGFBP-3 induces phosphorylation of c-JNK and suppression of Akt phosphorylation. 22RV1 CaP cells were incubated in serum-free media for 24 h in the presence or absence of 1 μg/ml IGFBP-3. Experiments were repeated three times. (**A**) Western immunoblot for phospho- and total Akt. (**B**) Akt kinase assay as assessed by phosphorylation of a GSK-3 fusion protein after immunoprecipitation of Akt. (**C**) Western immunoblot of phospho- and total JNK. H_2O_2 was used as a positive control for p-JNK activation. Experiments were repeated three times.

following: (i) dramatic tumor suppressive effects by a non-IGF-binding mutant of IGFBP-3, (ii) observation that autocrine/paracrine IGFBP-3 expression correlated with tumor suppression, rather than circulating serum levels, and (iii) no obvious effect of IGFBP-3 on non-cancerous tissues. IGFBP-3 transgenic mice have been described to be modestly growth restricted and glucose intolerant, in mechanisms that may be largely related to IGF inhibition (22). However, *in vitro* evidence would suggest that this too may also involve IGF-independent effects (23). It is probable that growth inhibiting and apoptosis-promoting effects by IGFBP-3 in the whole animal involve IGF-dependent and -independent mechanisms and both are major contributors to tumor suppression.

Although we have demonstrated using the Nur77 KO MEFs that a significant portion of IGFBP-3-induced caspase activation is Nur77 dependent, we were able to show a small but significant contribution that is Nur77 independent. This may be a cell type-specific phenomena or may involve activation of other various pathways that have been described for IGFBP-3 including the following: (i) activation of caspase 8 and 9 (24), (ii) cell-surface receptors (25), (iii) Stat1 activation (26), (iv) SMAD inhibition (27), (v) phosphatase activation (28) and (vi) calcium flux regulation (29).

In addition to IGFBP-3, Nur77-dependent apoptosis is induced by retinoid-related molecules (30,31), calcium ionophores and etoposide (30), which are known to act via signaling pathways that involve kinases and phosphatases. Indirect inactivation of survival kinases by different agents are used to elicit tumor death (32,33). A recent report implicates both activation of JNK and inhibition of Akt as necessary in translocation of Nur77 from the nucleus to the cytoplasm in other cancer models (18). We describe herein JNK activation and inhibition of Akt phosphorylation and activity by IGFBP-3, which translocates RXR/Nur77 in an IGF-independent manner (5). Other pro-apoptotic agents, such as oridonin (34), the multikinase inhibitor, sorafenib, and the proteasome inhibitor, bortezomib (35), have also been described to inhibit Akt and phosphorylate JNK, it is intriguing to speculate that Nur77 translocation may be involved as well.

Additional kinase pathways phosphorylate Nur77 including the mitogen-activated protein kinase pathway (36) and ribosomal S6 kinase and mitogen- and stress-activated kinase (37). We and others

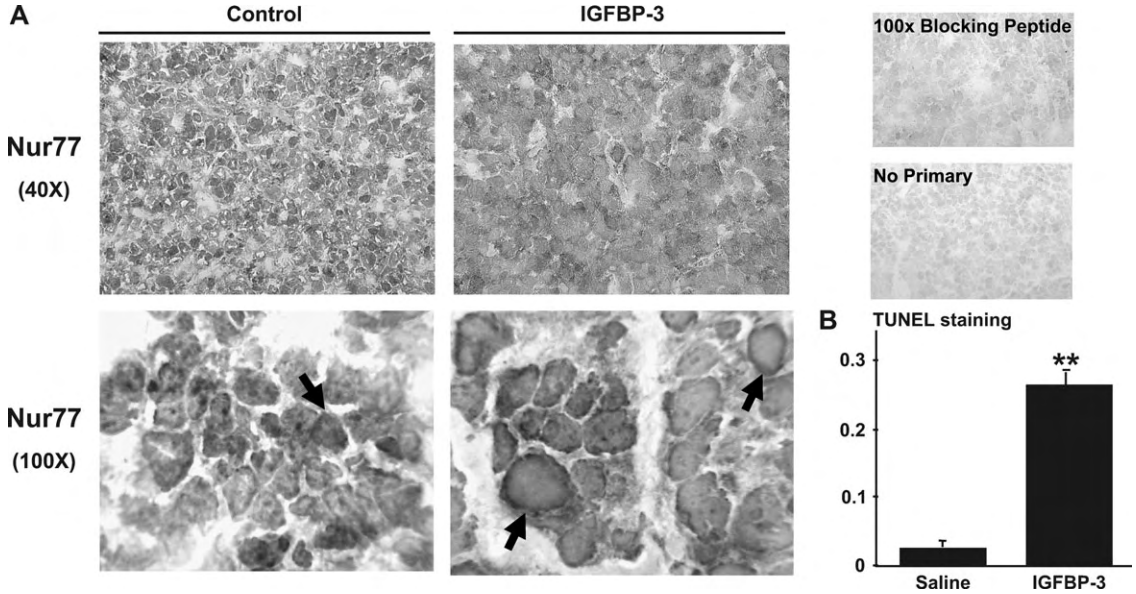

Fig. 5. IGFBP-3-induced apoptosis involves translocation of Nur77 in CaP xenografts *in vivo*. (**A**) Cross-sectioned LAPC-4 tumors stained with anti-Nur77 (×100, oil immersion). Diaminobenzidine was used as a chromogen (dark brown) and commercial hematoxylin was used for counterstaining (blue nuclei). Note predominant nuclear Nur77 staining in control tumor versus empty blue nuclei in the IGFBP-3-treated tumor. Top panel is ×40 magnification; lower panel is ×100 magnification (oil immersion). Arrows indicate nuclei in which Nur77 is intra-nuclearly stained or translocated to the mitochondria. Control immunohistochemistry shows competition of signal by blocking peptide, as well as lack of binding of secondary antibody. (See Supplementary material, available at *Carcinogenesis* Online, for coloured figure.) (**B**) Quantitation of TUNEL staining was used as a measure of apoptosis. TUNEL staining was quantitated by pixel histogram as indicated in bar graph. $^{**}P < 0.005$ relative to control treatment.

have additionally identified DNA protein kinase to phosphorylate IGFBP-3 *in vivo* and that this phosphorylation regulates nuclear localization (38,39). Additionally, casein kinase-2 has been shown to phosphorylate and negatively regulate IGFBP-3 (40). Complex kinase networks that control phosphorylation of both Nur77 and IGFBP-3 underscore the importance of multiple regulatory levels to determine activity of both these molecules and their subcellular localization.

In summary, the current work and previous work done by our group shows that IGFBP-3 is secreted and reuptaken by endocytic mechanisms to the nucleus (12). In the nucleus it interacts with the nuclear receptor RXR, where binding may expose a nuclear export sequence described previously in the DNA-binding domain of RXR (41) and indirectly enhance Nur77 binding to RXR (5). Conformation of this complex may further be changed after export to the cytoplasm where IGFBP-3 directly interacts with Nur77 as described in the current study. Immunohistochemical demonstration of the ability of IGFBP-3 to translocate Nur77 *in vivo* offers an output measure to assess IGFBP-3 efficacy in the clinical arena. Further work, including mitochondrial targeting of this complex, is needed to unravel the molecular mechanisms of IGFBP-3 intracellular activity and its potential clinical application.

Supplementary material

Supplementary figure can be found at http://carcin.oxfordjournals.org/.

Acknowledgements

The authors wish to thank David Hwang and George Lin for expert technical assistance. We are also grateful to Dr X.-k.Zhang for providing the Nur77 coding sequence. This work was supported in part by a CaP Foundation award and National Institutes of Health Grants RO1AG20954, P50CA92131 and RO1CA100938 (to P.C.); grants from the Stein-Oppenheimer Foundation, the Lawson Wilkins Pediatric Endocrinology Society, University of California, Los Angeles, CaP SPORE Career Development Award, National Institutes of Health Grant 2K12HD34610 (to K.-W.L.) and a Department of Defense awards PC050754 (to L.J.C) and PC061077 (to K.-W.L.).

Conflict of Interest Statement: None declared.

References

1. Chan,J.M. *et al*. (1998) Plasma insulin-like growth factor-I and prostate cancer risk: a prospective study. *Science*, **279**, 563–566.
2. Ali,O. *et al*. (2003) Epidemiology and biology of insulin-like growth factor binding protein-3 (IGFBP-3) as an anti-cancer molecule. *Horm. Metab. Res.*, **35**, 726–733.
3. Liu,B. *et al*. (2005) Combination therapy of insulin-like growth factor binding protein-3 and retinoid X receptor ligands synergize on prostate cancer cell apoptosis *in vitro* and *in vivo*. *Clin. Cancer Res.*, **11**, 4851–4856.
4. Silha,J.V. *et al*. (2006) Insulin-like growth factor binding protein-3 attenuates prostate tumor growth by IGF-dependent and IGF-independent mechanisms. *Endocrinology*, **147**, 2112–2121.
5. Lee,K.W. *et al*. (2005) Rapid apoptosis induction by IGFBP-3 involves an insulin-like growth factor-independent nucleomitochondrial translocation of RXRalpha/Nur77. *J. Biol. Chem.*, **280**, 16942–16948.
6. Lin,B. *et al*. (2004) Conversion of Bcl-2 from protector to killer by interaction with nuclear orphan receptor Nur77/TR3. *Cell*, **116**, 527–540.
7. Moll,U.M. *et al*. (2006) p53 and Nur77/TR3-transcription factors that directly target mitochondria for cell death induction. *Oncogene*, **25**, 4725–4743.
8. Craft,N. *et al*. (1999) A mechanism for hormone-independent prostate cancer through modulation of androgen receptor signaling by the HER-2/neu tyrosine kinase. *Nat. Med.*, **5**, 280–285.
9. Sell,C. *et al*. (1993) Simian virus 40 large tumor antigen is unable to transform mouse embryonic fibroblasts lacking type 1 insulin-like growth factor receptor. *Proc. Natl Acad. Sci. USA*, **90**, 11217–11221.
10. Liu,B. *et al*. (2000) Direct functional interactions between insulin-like growth factor-binding protein-3 and retinoid X receptor-alpha regulate transcriptional signaling and apoptosis. *J. Biol. Chem.*, **275**, 33607–33613.
11. Schedlich,L.J. *et al*. (2004) Insulin-like growth factor binding protein-3 prevents retinoid receptor heterodimerization: implications for retinoic acid-sensitivity in human breast cancer cells. *Biochem. Biophys. Res. Commun.*, **314**, 83–88.
12. Lee,K.W. *et al*. (2004) Cellular internalization of insulin-like growth factor binding protein-3: distinct endocytic pathways facilitate re-uptake and nuclear localization. *J. Biol. Chem.*, **279**, 469–476.
13. Weih,F. *et al*. (1996) Apoptosis of nur77/N10-transgenic thymocytes involves the Fas/Fas ligand pathway. *Proc. Natl Acad. Sci. USA*, **93**, 5533–5538.
14. Cheng,L.E. *et al*. (1997) Functional redundancy of the Nur77 and Nor-1 orphan steroid receptors in T-cell apoptosis. *EMBO J.*, **16**, 1865–1875.
15. Kolluri,S.K. *et al*. (2003) Mitogenic effect of orphan receptor TR3 and its regulation by MEKK1 in lung cancer cells. *Mol. Cell. Biol.*, **23**, 8651–8667.
16. Masuyama,N. *et al*. (2001) Akt inhibits the orphan nuclear receptor Nur77 and T-cell apoptosis. *J. Biol. Chem.*, **276**, 32799–32805.
17. Pekarsky,Y. *et al*. (2001) Akt phosphorylates and regulates the orphan nuclear receptor Nur77. *Proc. Natl Acad. Sci. USA*, **98**, 3690–3694.
18. Han,Y.H. *et al*. (2006) Regulation of Nur77 nuclear export by c-Jun N-terminal kinase and Akt. *Oncogene*, **25**, 2974–2986.
19. Oufattole,M. *et al*. (2006) *et al*. (2006) Rna polymerase II binding subunit 3 (rpb3), a potential nuclear target of IGFBP-3. *Endocrinology*, **147**, 2138–2146.
20. Ikezoe,T. *et al*. (2004) Insulin-like growth factor binding protein-3 antagonizes the effects of retinoids in myeloid leukemia cells. *Blood*, **104**, 237–242.
21. Schedlich,L.J. *et al*. (1998) Insulin-like growth factor-binding protein (IGFBP)-3 and IGFBP-5 share a common nuclear transport pathway in T47D human breast carcinoma cells. *J. Biol. Chem.*, **273**, 18347–18352.
22. Silha,J.V. *et al*. (2002) Impaired glucose homeostasis in insulin-like growth factor-binding protein-3-transgenic mice. *Am. J. Physiol. Endocrinol. Metab.*, **283**, E937–E945.
23. Chan,S.S. *et al*. (2005) Insulin-like growth factor binding protein-3 leads to insulin resistance in adipocytes. *J. Clin. Endocrinol. Metab.*, **90**, 6588–6595.
24. Bhattacharyya,N. *et al*. (2006) Nonsecreted insulin-like growth factor binding protein-3 (IGFBP-3) can induce apoptosis in human prostate cancer cells by IGF-independent mechanisms without being concentrated in the nucleus. *J. Biol. Chem.*, **281**, 24588–24601.
25. Huang,S.S. *et al*. (2003) Cellular growth inhibition by IGFBP-3 and TGF-beta1 requires LRP-1. *FASEB J.*, **17**, 2068–2081.
26. Spagnoli,A. *et al*. (2002) Identification of STAT-1 as a molecular target of insulin-like growth factor binding protein-3 (IGFBP-3) in the process of chondrogenesis. *J. Biol. Chem.*, **277**, 18860–18867.
27. Fanayan,S. *et al*. (2002) Signaling through the Smad pathway by insulin-like growth factor-binding protein-3 in breast cancer cells. Relationship to transforming growth factor-beta 1 signaling. *J. Biol. Chem.*, **277**, 7255–7261.
28. Ricort,J.M. *et al*. (2002) Insulin-like growth factor-binding protein-3 activates a phosphotyrosine phosphatase. Effects on the insulin-like growth factor signaling pathway. *J. Biol. Chem.*, **277**, 19448–19454.
29. Ricort,J.M. *et al*. (2002) Insulin-like growth factor binding protein-3 increases intracellular calcium concentrations in MCF-7 breast carcinoma cells. *FEBS Lett.*, **527**, 293–297.
30. Li,H. *et al*. (2000) Cytochrome c release and apoptosis induced by mitochondrial targeting of nuclear orphan receptor TR3. *Science*, **289**, 1159–1164.
31. Dawson,M.I. *et al*. (2001) Apoptosis induction in cancer cells by a novel analogue of 6-[3-(1-adamantyl)-4-hydroxyphenyl]-2-naphthalenecarboxylic acid lacking retinoid receptor transcriptional activation activity. *Cancer Res.*, **61**, 4723–4730.
32. Kawauchi,K. *et al*. (2003) Involvement of Akt kinase in the action of STI571 on chronic myelogenous leukemia cells. *Blood Cells Mol. Dis.*, **31**, 11–17.
33. Sordella,R. *et al*. (2004) Gefitinib-sensitizing EGFR mutations in lung cancer activate anti-apoptotic pathways. *Science*, **305**, 1163–1167.
34. Jin,S. (2007) Oridonin induced apoptosis through Akt and MAPKs signaling pathways in human osteosarcoma cells. *Cancer Biol. Ther.*, **6**, 261–268.
35. Yu,C. *et al*. (2006) Cytotoxic synergy between the multikinase inhibitor sorafenib and the proteasome inhibitor bortezomib *in vitro*: induction of apoptosis through Akt and c-Jun NH2-terminal kinase pathways. *Mol. Cancer Ther.*, **5**, 2378–2387.
36. Katagiri,Y. *et al*. (2000) Modulation of retinoid signalling through NGF-induced nuclear export of NGFI-B. *Nat. Cell Biol.*, **2**, 435–440.
37. Wingate,A.D. *et al*. (2006) Nur77 is phosphorylated in cells by RSK in response to mitogenic stimulation. *Biochem. J.*, **393**, 715–724.
38. Cobb,L.J. *et al*. (2006) Phosphorylation by DNA-dependent protein kinase is critical for apoptosis induction by insulin-like growth factor binding protein-3. *Cancer Res.*, **66**, 10878–10884.

39. Schedlich,L.J. *et al*. (2003) Phosphorylation of insulin-like growth factor binding protein-3 by deoxyribonucleic acid-dependent protein kinase reduces ligand binding and enhances nuclear accumulation. *Endocrinology*, **144**, 1984–1993.
40. Coverley,J.A. *et al*. (2000) The effect of phosphorylation by casein kinase 2 on the activity of insulin-like growth factor-binding protein-3. *Endocrinology*, **141**, 564–570.
41. Cao,X. *et al*. (2004) Retinoid X receptor regulates Nur77/TR3-dependent apoptosis [corrected] by modulating its nuclear export and mitochondrial targeting. *Mol. Cell. Biol.*, **24**, 9705–9725.

Received September 13, 2006; revised February 28, 2007; accepted March 29, 2007

0031-3998/07/6102-0159
PEDIATRIC RESEARCH
Vol. 61, No. 2, 2007
Printed in U.S.A.

Insulin-Like Growth Factor Binding Protein-3 Induces Insulin Resistance in Adipocytes *In Vitro* and in Rats *In Vivo*

HAE SOON KIM, OMAR ALI, MELANIE SHIM, KUK-WHA LEE, PATRICIA VUGUIN, RADHIKA MUZUMDAR, NIR BARZILAI, AND PINCHAS COHEN

Department of Pediatrics [H.S.K.], Ewha Womans University, Seoul, 120-750 Korea; David Geffen School of Medicine [O.A., M.S., K.-W.L., P.C.], University of California–Los Angeles, Los Angeles, California 90095; Albert Einstein College of Medicine [P.V., R.M., N.B.], Bronx, New York 10461

ABSTRACT: Insulin-like growth factor binding protein (IGFBP)-3 binds to IGF and modulates their actions and also possesses intrinsic activities. We investigated its effects on insulin action and found that when IGFBP-3 was added to fully differentiated 3T3-L1 adipocytes in culture, insulin-stimulated glucose transport was significantly inhibited to 60% of control in a time- and dose-dependent manner. Tumor necrosis factor (TNF)-α treatment also inhibited glucose transport to the same degree as IGFBP-3 and, in addition, increased IGFBP-3 levels 3-fold. Co-treatment with TNF-α and IGFBP-3 antisense partially prevented the inhibitory effect of TNF-α on glucose transport, indicating a role for IGFBP-3 in cytokine-induced insulin resistance. Insulin-stimulated phosphorylation of the insulin receptor was markedly decreased by IGFBP-3 treatment. IGFBP-3 treatment suppressed adiponectin expression in 3T3-L1 adipocytes. Infusion of IGFBP-3 to Sprague-Dawley rats for 3 h decreased peripheral glucose uptake by 15% compared with controls as well as inhibiting glycogen synthesis. Systemic administration of IGFBP-3 to rats for 7 d resulted in a dramatic 40% decrease in peripheral glucose utilization and glycogen synthesis. These *in vitro* and *in vivo* findings demonstrate that IGFBP-3 has potent insulin-antagonizing capability and suggest a role for IGFBP-3 in cytokine-induced insulin resistance and other mechanisms involved in the development of type-2 diabetes. **(*Pediatr Res* 61: 159–164, 2007)**

IGF-I and -II are involved in the regulation of cell growth and differentiation in a variety of cell types (1). However, the IGF also mimic some of the metabolic actions of insulin and act as insulin sensitizers (2). IGF-I has approximately 1/12th the glucose-lowering capacity of insulin (3), *in vivo* and an equipotent effect on *ex vivo* muscle strips (4), as well as being an insulin sensitizer, and has been considered as a putative treatment agent for both type-1 and type-2 diabetes (5,6). The IGFBP are a family of six binding proteins that bind to IGF with high affinity and specificity. A variety IGFBP profiles are observed in different tissues, presumably regulating specific cellular activities. IGFBP-3 is the most abundant circulating IGF binding protein and is expressed in most tissues. IGFBP-3 not only regulates IGF bioavailability and action (so-called IGF-dependent actions), but also mediates IGF independent actions on cell survival and apoptosis (7–9). By binding IGF in the circulation, the IGFBP reduce the levels of free IGF and antagonize their insulin-like activity; in addition, they may be involved in carbohydrate metabolism in ways that remain poorly characterized (10). IGFBP-3 levels are regulated by multiple factors, including cytokines that have been implicated in insulin resistance, such as TNF-α. Recently, it has been shown that IGFBP-3 reduces insulin-stimulated glucose uptake in both rodent and human adipocytes (11). We carried out a series of experiments to elucidate the effects of IGFBP-3 on insulin sensitivity *in vitro* and *in vivo* and the mechanisms involved in its actions. In addition, we show here that the insulin-antagonistic effects of tumor necrosis factor (TNF)-α are mediated in part by IGFBP-3.

MATERIALS AND METHODS

Materials. Recombinant hIGFBP-3 was a generous gift from Celtrix (Mountain View, CA). Human recombinant insulin was obtained from Sigma Chemical Co. (Saint Louis, MO). 2-[3H (G)] deoxy-D-glucose was purchased from New England Nuclear, Inc. (Boston, MA). Anti-human IGFBP-3 antibodies, which were affinity purified on an IGFBP-3 column, were purchased from Diagnostic Systems Laboratories (Webster, TX). 125-I-labeled IGF-I and IGF-II were purchased from Amersham (Piscataway, NJ). Anti-phospho-insulin receptor beta subunit antibody was purchased from BioSource International (Camarillo, CA). Anti-adiponectin antibody was purchased from Chemicon International (Temecula, CA) The Bradford protein assay kit and all electrophoresis chemicals were obtained from Bio-Rad (Richmond, CA). All other chemicals were purchased form Sigma Chemical Co. The antisense oligonucleotide designed to flank the initiation codon of murine IGFBP-3 (12) was GCGCGCGGGATGCATGGCGCCGGGTGGACG, with the corresponding sense oligonucleotide being 5′- CGTCCAC-CCGGCGCCATG-CATCCCGCGCGC. Thio-ester bonds linked the first three and final three nucleotides of each oligo (Sigma-Genosys, Ltd., The Woodlands, TX).

Cell culture. All cell lines and tissue culture reagents were purchased from ATCC (Rockville, MD). 3T3-L1 adipocytes were cultured in Dulbecco's modified Eagle's medium (DMEM) supplemented with 10% fetal bovine serum (FBS) and an antibiotic mixture containing penicillin and streptomycin. For the experiments, cells were cultured in 12-well dishes and differentiated into adipocytes using 3-isobutyl 1-methylxanthine, dexamethasone and insulin, according to methods previously described (13). Briefly, confluent cultures were incubated with the differentiation medium containing dexamethasone (25 μM), isobutyl methylxanthine (0.5 mM), and insulin (100 nmol/L) in DMEM with 10% FBS for 48 h. The cells were then maintained in a medium containing 10% FBS and insulin (10nmol/L). Experiments were performed when greater than 90% of the cells were differentiated into adipocytes.

Received July 27, 2006; accepted September 5, 2006.

Correspondence: Pinchas Cohen, M.D., Division of Pediatric Endocrinology, David Geffen School of Medicine at UCLA, 10833 Le Conte Ave., MDCC 22-315, Los Angeles, CA 90095-1752; e-mail: hassy@mednet.ucla.edu

Supported, in part, by National Institutes of Health grants R01AG20954, R01HD047013, P50CA92131, P30DK063491 (to PC), and P01-AG021654 (to NB).

DOI: 10.1203/pdr.0b013e31802d8a30

Abbreviations: IGFBP, insulin-like growth factor binding protein; **PPAR,** peroxisome proliferator activated receptor

Glucose transport assay. Before glucose transport assays, the cells were incubated in serum-free media, with or without treatment (IGFBP-3 or TNF-α). Treatment with IGFBP-3 was performed at various concentrations and durations (see "Results"). TNF-α treatment was performed at a concentration of 10 ng/mL for 24 h. All experiments were done in triplicate unless otherwise indicated. The procedure for glucose transport measurement was modified from methods previously described (14). After the treatment period, the cells were washed twice with PBS and incubated in the same buffer for 30 min with insulin (10 nmol/L). The transport reaction was started by addition of 10 μL substrate (3H-2-deoxyglucose 0.1 μCi to produce a final concentration of 0.1 mM) and halted after 5 min by aspirating the reaction mixture and rapidly rinsing each well five times with 4-degree PBS. Cells were solubilized by addition of 0.5 mL 0.1 N NaOH and incubated with shaking. An aliquot (100 μL) of the suspension was removed for protein analysis using Bio-Rad reagent (Richmond, CA) (15). After solubilization, 400 μL of the suspension was placed in a scintillation vial and neutralized with 1.0 N HCL and scintillation fluid was added. Radioactivity in this lysate was determined by scintillation counting.

Western immunoblots. Phosphorylated insulin receptor beta subunit levels were detected using cell lysate from differentiated 3T3-L1 adipocytes that were treated with or without IGFBP-3 (1 μg/mL) for 24 h. Each of these experiments was performed in the presence or absence of insulin (10 nmol/L) for the last 30 min of the treatment period. Adiponectin was detected using cell lysates from 3T3-L1 adipocytes that were treated with or without IGFBP-3 (1 μg/mL) and rosiglitazone (10 μM/L) for 24 h. All experiments were repeated three times. Samples of 50 μL were separated by nonreducing 8% SDS-PAGE overnight at constant voltage and electroblotted onto nitrocellulose. The membranes were then sequentially washed with NP40, 1%BSA, and Tween 20, blocked with 5% nonfat dry milk in Tris-buffered saline, probed with the specified antibody and detected using a peroxidase-linked enhanced chemiluminescence detection system (Amersham, Arlington Heights, IL).

Immunofluorescence confocal microscopy. Fully differentiated 3T3-L1 adipocytes, 1×10^4, were plated on cover-glass in serum containing media for 2 d. The cells were then incubated in serum-free medium for 24 h. For the last 6 h, half of the wells were treated with IGFBP-3 in a dose of 1 μg/mL for 6 h. The cells were then exposed to insulin (10 nmol/L) for 30 min. After three washes in PBS, fixation and permeabilization of the cells were performed with 1% paraformaldehyde in PBS for 15 min at room temperature and 0.2% Triton X-100 in PBS for 15 min on ice, and cells were washed twice with PBS. Specimens were incubated with primary antibodies in PBS for 1 h at room temperature, with secondary antibodies in PBS for 40 min at room temperature, and then incubated with Hoechst from Electron Microscopy Sciences (Ft. Washington, PA) for 2 min. Samples were analyzed using the Inverted Confocal Microscope (Leica, Wetzlar, Germany), equipped by digital camera (Hamamatsu, Hamamatsu City, Japan), and operated by QED-image software. DAPI (blue) identifies the nuclei.

To examine IGFBP-3 induction by TNF-α, 1×10^4 fully differentiated 3T3-L1 adipocytes were plated on cover-glass in serum containing media for 2 d. The cells were then incubated in serum-free media with or without TNF-α at a concentration of 10 ng/mL for 48 h, before staining for immunofluorescence as described above. IGFBP-3 protein localization was detected using the DSL hIGFBP-3 goat polyclonal antibody (which was previously purified on an IGFBP-3 column), diluted 1:200, followed by fluorescein anti-goat antibody (Vector Laboratories, Burlingame, CA). Samples were then analyzed using the Inverted Confocal Microscope at 60$\times$ magnification (Leica), equipped by digital camera (Hiramitsu), and operated by QED-image software.

Western ligand blotting. IGFBP-3 protein levels were assessed using cell lysate from 3T3-L1 adipocytes that were treated with or without TNF-α (10 ng/mL) for 48 h. Samples of 50 μL were separated by nonreducing 10% SDS-PAGE overnight at constant voltage and electroblotted onto nitrocellulose. The membranes were then sequentially washed with NP40, 1% BSA, and Tween 20, incubated with 106 cpm each of ^{125}I-labeled IGF-I and IGF-II for 12 h, dried, and exposed to film for 5 d. All experiments were done in triplicate.

IGFBP-3 antisense treatment. 3T3-L1 adipocytes were grown and differentiated in 12-well plates (in quadruplicates) as described above. The cells were then preincubated with sense or antisense IGFBP-3 oligos (detailed above), at concentrations of 500 ng/plate for 30 min in the presence of LipofectAMINE (Invitrogen). Following the preincubation, the cells were incubated in serum-free medium for 24 h with and without TNF-α (10 ng/mL). At the end of the 24 h, the cells were treated with insulin (10 nmol/L) and a glucose transport assay was performed as described above.

In vivo hyperinsulinemic euglycemic clamps. The principles of laboratory animal care set out by the National Institutes of Health were followed strictly. The study protocol was reviewed and approved by the Animal Care and Use Committee of the Albert Einstein College of Medicine. Male Sprague-Dawley rats (Charles River Laboratories, Wilmington, MA) were housed in individual cages and subjected to a standard light (0600–1800 h) and dark (1800–0600 h) cycle. They were fed *ad libitum* using regular rat chow that consisted of 64% carbohydrate, 30% protein, and 6% fat with a physiologic fuel value of 3.3 kcal/g chow.

To study the acute effects of an infusion of IGFBP-3, two groups of awake, unstressed, chronically catheterized Sprague-Dawley rats (0.3 kg) were studied for 300 min. All rats received a primer continuous infusion (15–49 μCi/min bolus, 0.4 μCi/min) of [3-3H] glucose throughout the study. After establishing rates of basal glucose turnover, a primed infusion of somatostatin (1.5 μg/kg/min), insulin (3 mU/kg/min), and a variable infusion of 25% glucose to clamp the plasma concentration of euglycemic levels of 140 mg/dL was administered for 2 h. At 120 min, the rats received a primed continuous infusion of IGFBP-3 (60 μg/kg/h) or saline (control) for an additional 3 h.

For the chronic IGFBP-3 infusion experiments, Sprague-Dawley rats (0.3 kg) received either IGFBP-3 (40 μg/kg/h) or saline as control by osmotic minipumps for 7 d and clamp studies were performed on d 7. All rats received a primed continuous infusion (15–49 μCi/min bolus, 0.4 μCi/min) of [3-3H] glucose throughout the study. After establishing rates of basal glucose turnover, a primed infusion of somatostatin (1.5 μg/kg/min), insulin (3 mU/kg/min), and a variable infusion of 25% glucose to clamp the plasma glucose concentration at euglycemic levels of 140 mg/dL were administered for 2 h. Recombinant human IGFBP-3 levels in rat sera were measured by ELISA (DSL, Webster, TX). There was no cross-reactivity between human and rat IGFBP-3 in this assay.

Statistical analysis. Statistical significance was evaluated using *t* tests and ANOVA and two-tailed *p* values were calculated. Significance was accepted at the $p < 0.05$ level.

RESULTS

IGFBP-3 inhibits glucose uptake in 3t3-L1 adipocytes. Addition of 1 μg/mL IGFBP-3 to 3T3 adipocytes for 24 h resulted in a >40% decrease in insulin-stimulated glucose transport compared with serum-free controls. When adipocytes were exposed to IGFBP-3 for 24 h at a concentration of 1 μg/mL, glucose transport decreased by >40% (Fig. 1*A*). This is similar to the decrease in insulin-stimulated glucose transport observed when adipocytes are exposed to 10 ng/mL TNF-α over the same time period.

Treatment with IGFBP-3 for 24 h suppressed glucose uptake in adipocytes in a dose-dependent manner. The effect was maximal at an IGFBP-3 concentration of 1 μg/mL where glucose transport decreased by 40% compared with serum-free controls. Treatment with IGFBP-3 at a concentration of 1.5 μg/mL did not increase the response (Fig. 1*B*). In addition, a time course treatment with IGFBP-3 at a concentration of 1 μg/mL demonstrated suppression of glucose uptake in a time-dependent manner. The suppression was greatest after 24 h of treatment; however, an effect was detectable as early as 30 min of treatment (Fig. 1*C*). These results indicate that IGFBP-3 induces insulin resistance *in vitro*, in a time- and dosage-dependent manner. IGFBP-3 inhibited basal glucose transport by 20% (Fig. 1*D*).

TNF-α induces the production of IGFBP-3 in 3T3-L1 adipocytes. To test whether TNF-α induces IGFBP-3 production in 3T3-L1 adipocytes, adipocytes in serum-free media were treated with TNF-α for 48 h at a concentration of 10 ng/mL. Production of IGFBP-3 was then detected by immunofluorescence confocal microscopy using a rodent IGFBP-3-specific antibody. Following TNF-α treatment, the overall levels of IGFBP-3, (stained in green) in the cells rose dramatically compared with serum-free controls (Fig. 2), implying increased endogenous production. Interestingly, IGFBP-3 lo-

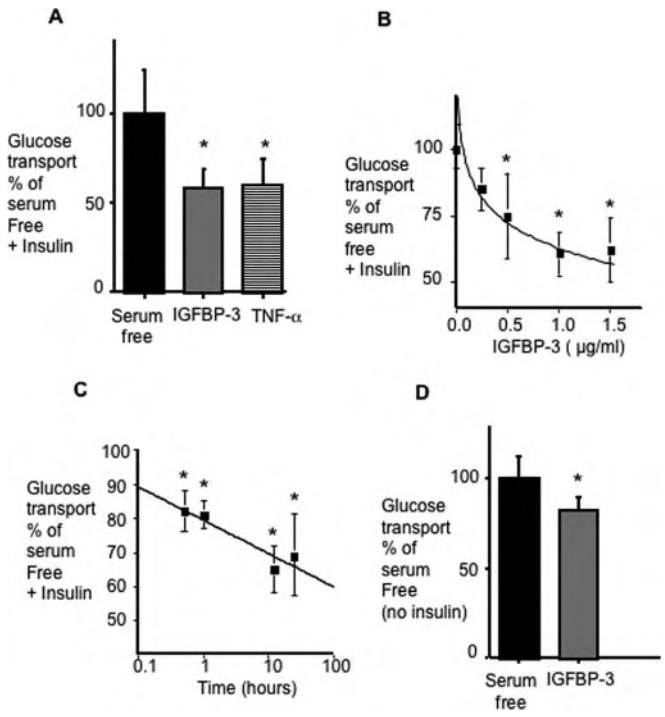

Figure 1. Effect of IGFBP-3 on insulin-stimulated glucose uptake in 3T3-L1 adipocytes. (*A*) 3T3-L1 adipocytes treated ($n = 3$ per condition) with 1 μg/mL IGFBP-3 or with 10 ng/mL TNF-α for 24 h and pulsed with insulin (10 nmol/L) $\times$30 min before measurement of glucose transport as described. Glucose transport expressed as percentage of serum-free conditions. Dose response (*B*) and time course (*C*) are also shown. The effects of 1 μg/mL IGFBP-3 on basal glucose transport ($n = 4$ per group) are shown in (*D*). *$p < 0.05$.

cated within the nuclei at low levels in basal conditions appears to increase to a greater extent in response to treatment with TNF-α.

The increase in IGFBP-3 protein levels in response to treatment with TNF-α was also demonstrated by densitometric analysis of Western ligand blots using ^{125}I-IGF-I and -II. We quantified the protein levels of IGFBP-3 in total cell lysates of adipocytes that were exposed to treatment with TNF-α at a concentration of 10 ng/mL for 72 h. When the blot was assessed by densitometric analysis, it was found that TNF-α induced a 3-fold increase in production of IGFBP-3 compared with serum-free conditions ($p < 0.05$, Fig. 2*B*).

Insulin-antagonistic effect of TNF-α is partially blocked by pretreatment with IGFBP-3 antisense. To test whether the insulin-antagonistic action of TNF-α may be mediated *via* induction of IGFBP-3, 3T3-L1 adipocytes were exposed to TNF-α after transfection of IGFBP-3 antisense or sense oligonucleotides. Cells pretreated with antisense IGFBP-3 oligos and then treated with TNF-α 10 ng/mL exhibited a significantly smaller decrease in insulin-mediated glucose transport ($p < 0.05$, Fig. 2*C*). Cell extracts transfected with antisense IGFBP-3 demonstrate >50% reduction in IGFBP-3 content by immunoblot with no change noted in the sense-transfected cells.

IGFBP-3 inhibits insulin-receptor-phosphorylation in 3T3-L1 adipocytes. To examine whether IGFBP-3 induces insulin resistance by decreasing the tyrosine phosphorylation of insulin receptors on the cell membrane, phosphorylated insulin receptor levels were assayed. Cells were treated with and without IGFBP-3 (1 μg/mL) for 24 h in serum-free media. Each of these conditions was performed in the presence or absence of insulin (10 nmol/L) for the final 30 min of the treatment period. Western blotting of phosphorylated insulin receptor beta subunit proteins from these insulin-treated cells, which were also treated with IGFBP-3, revealed a 70% decrease in insulin-stimulated phosphorylation of the insulin receptor compared with cells treated with insulin alone (Fig. 3).

IGFBP-3 inhibit adiponectin expression in mature adipocyte. To determine whether IGFBP-3 regulates additional adipocyte functions, we examined the effects of IGFBP-3 on

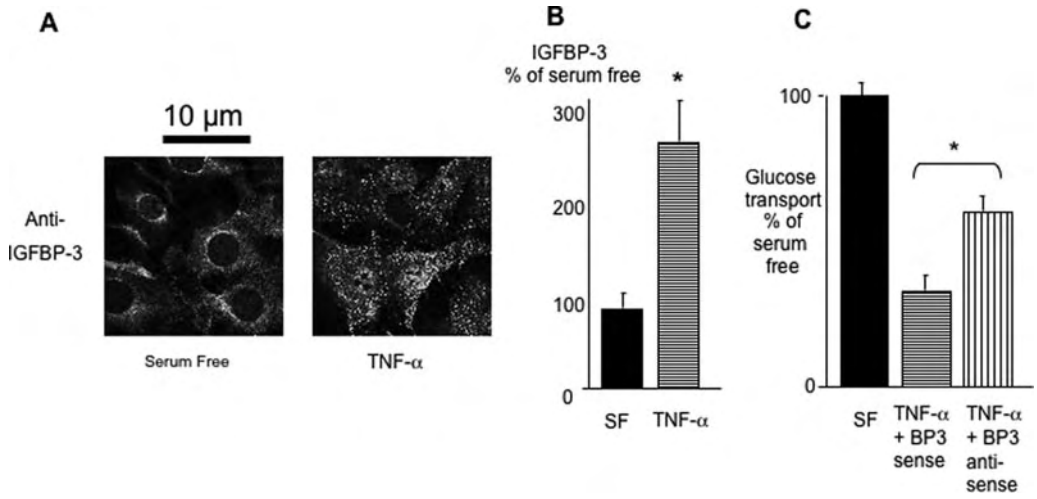

Figure 2. Exposure to TNF-α induces IGFBP-3 production in 3T3-L1 adipocytes that is involved in glucose transport regulation. (*A*) Confocal microscopy of 3T3-L1 adipocytes in culture treated with TNF-α (10 ng/mL) $\times$ 48 h, then stained with IGFBP-3 antibody and counterstained with fluorescein-labeled anti-rabbit antibody before confocal microscopy. (*B*) Cells similarly treated with TNF-α (10 ng/mL) $\times$ 72 h were lysed and IGFBP-3 content was assayed using Western-ligand blotting and quantified densitometrically. (*C*) 3T3-L1 adipocytes were pretreated with IGFBP-3 sense and antisense oligos ($n = 4$ per group) for 30 min as described. They were then treated with TNF-α 10 ng/mL for 24 h and pulsed with insulin 10nmol/L and glucose transport was assayed as described. Results are expressed as percentage of serum-free. *$p < 0.05$.

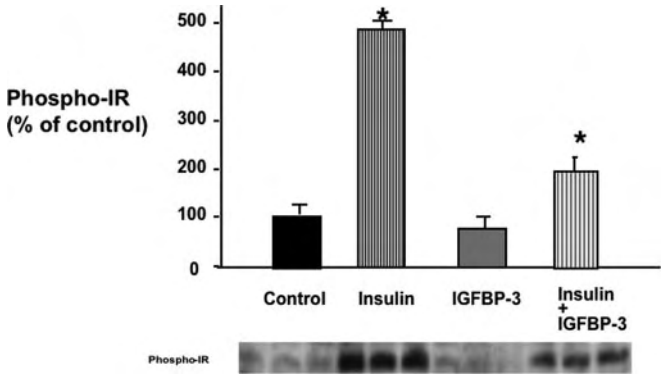

Figure 3. Effect of IGFBP-3 on insulin-stimulated phosphorylation of the insulin receptor. 3T3-L1 adipocytes ($n = 3$ per group) treated with 1 μg/mL IGFBP-3 for 24 h and pulsed with insulin (10 nmol/L) $\times$ 30 min. Cells were lysed and lysates were electrophoresed and blotted with phospho-specific insulin receptor antibody. Western blot densitometry was expressed as percent of SF. $^*p < 0.05$.

adiponectin expression. Adiponectin immunoblots were performed on cell lysates from differentiated 3T3-L1 adipocytes that were treated with and without IGFBP-3 and the PPARγ agonist rosiglitazone for 24 h in serum-free media. Western blotting of adiponectin from IGFBP-3 treated cells revealed a 55% decrease in adiponectin expression compared with control. PPARγ-stimulated adiponectin was also inhibited by IGFBP-3 (Fig. 4).

Infusion of IGFBP-3 impairs glucose metabolism in Sprague-Dawley rats. To examine the effect of elevated IGFBP-3 levels upon insulin sensitivity *in vivo*, we studied Sprague-Dawley rats utilizing the insulin clamp technique. Acute effects were studied by infusing IGFBP-3 (60 μg/kg/h) for 3 h. Because maximal effect *in vitro* is seen after several days, we also performed IGFBP-3 infusion for 7 d and the effects of prolonged exposure were studied by continuously infusing 40 μg/kg/h over 7 d.

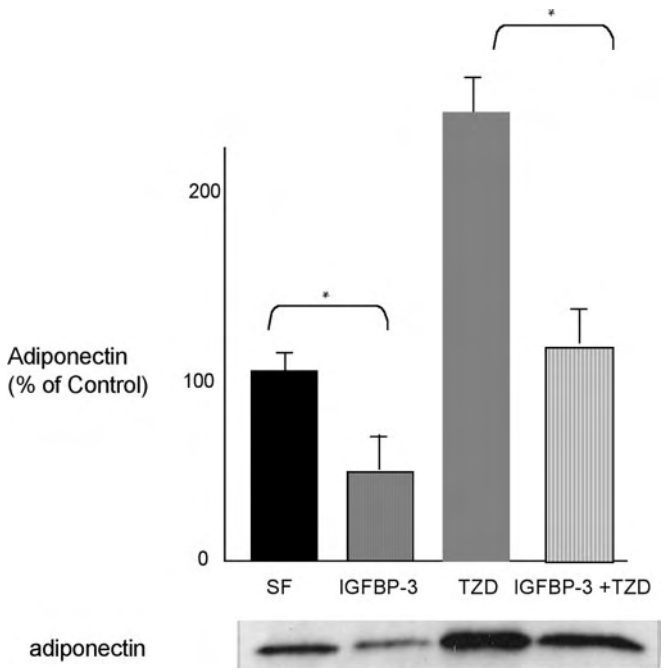

Figure 4. Effect of IGFBP-3 on adiponectin expression in 3T3-L1 adipocytes. 3T3-L1 adipocytes ($n = 3$ per group) treated with 1 μg/mL IGFBP-3 for 24 h with or without rosiglitazone. Cells were lysed and lysates were electrophoresed and blotted with adiponectin antibody. Western blot densitometry was expressed as percentage of control. $^*p < 0.05$.

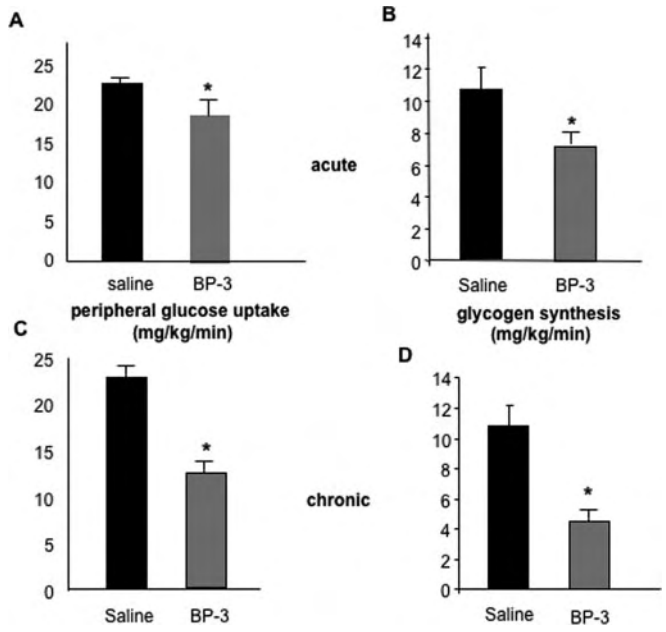

Figure 5. Effects of a 3 h infusion of IGFBP-3 (*A* and *B*) and of 7 d of IGFBP-3 infusion (*C* and *D*) on peripheral glucose uptake and glycogen synthesis in Sprague-Dawley rats. Rats ($n = 6$ per group) were infused with IGFBP-3 (60 μg/kg/h) for 3 h or with IGFBP-3 40 μg/kg/h for 7 d. Glucose uptake and glycogen synthesis were assayed as described. $^*p < 0.05$.

Infusion of IGFBP-3 for 3 h decreased peripheral glucose uptake by 15% compared with controls (19.0 $\pm$ 0.7 *versus* 22.8 $\pm$ 0.3 mg/kg/min, treatment *versus* control; $p < 0.05$). Glycogen synthesis was decreased by 25% (7.3 $\pm$ 0.3 mg/kg/min *vs* 10.8 $\pm$ 1.4, treatment *versus* control; $p < 0.05$) (Fig. 5, *A* and *B*).

Seven days of IGFBP-3 infusion decreased the peripheral glucose uptake (Rd) by 40% in rats treated with IGFBP-3 compared with control (14.0 $\pm$ 0.2 *versus* 23.2 $\pm$ 0.5 mg/kg/min, treatment *versus* control; $p < 0.01$). This decrease in Rd was primarily accounted for by a 50% decrease in glycogen synthesis (4.5 $\pm$ 1.0 *versus* 10.8 $\pm$ 1.4 mg/kg/min, treatment *versus* control; $p < 0.005$) (Fig. 5, *C* and *D*). Human IGFBP-3 levels were undetectable in preinfusion sera and achieved levels of 1200 $\pm$ 225 ng/mL at the end of 7 d, well within the physiologic range.

DISCUSSION

In this study, we have shown that IGFBP-3 rapidly induces insulin resistance *in vivo* and *in vitro* and that this effect occurs at physiologic concentrations of IGFBP-3. We have also demonstrated a link between IGFBP-3 induction and the insulin-antagonistic effect of inflammatory cytokines.

It has previously been shown that transgenic mice that over-express human IGFBP-3 cDNA exhibit fasting hyperglycemia, impaired glucose toleranc, and insulin resistance, without an apparent change in total IGF-I levels, and this was not

clearly explained by disturbances in growth hormone secretion or adiposity (16).

A relationship of elevated circulating IGFBP-3 levels to hyperglycemia is also suggested in certain clinical states characterized by impaired insulin action including puberty (17), acromegaly (18), and treatment with recombinant hGH (19). These conditions are associated with the development of insulin resistance and glucose intolerance despite a concomitant elevation of circulating IGF-I levels in each case. We show in this paper that IGFBP-3 is a potent insulin antagonist in 3T3-L1 adipocytes and in Sprague-Dawley rats. Our results also show that the magnitude of this effect is similar to the effect of TNF-α, a multifunctional cytokine that may be an important mediator of insulin resistance linked to obesity (20).

It was not directly tested in our studies whether IGFBP-3 insulin-antagonizing effects are dependent or independent of IGF-I. But Chan *et al.* (13) recently showed that IGFBP-3 mutants with reduced binding to IGF-I and -II were still able to reduce insulin-stimulated glucose uptake and both that group's as well as our data demonstrated that other IGFBP do not mediate this effect. This suggests the possibility that the inhibitory effect of IGFBP-3 may be independent of its binding to IGF, although an IGF-inhibitory mechanism is also possible. Distinguishing between these possibilities *in vivo* will require additional studies involving the systemic administration of non-IGF-binding mutants of IGFBP-3. Hyperglycemia has been convincingly demonstrated after the injection of IGFBP-1 (21) in rats and in transgenic mice, which overexpress IGFBP-1 (22), however, an IGF-dependent mechanism for this phenomena has been postulated.

IGFBP-3 in serum inhibits the effects of IGF on IGF-activated glucose consumption in mouse fibroblasts (23). In addition, glucose intolerance is observed in liver-specific IGF-I knockout mice (24) where circulating IGF-I levels are reduced to a larger degree than those of IGFBP-3. In these situations, the hyperglycemia could be attributable to a reduction in free IGF-I levels. It is possible that excess IGFBP-3 binds free (unbound) IGF-I, thereby decreasing its bioavailability and its hypoglycemic effect.

However, in addition to modulating the availability of IGF-I, IGFBP-3 has been shown to have independent effects in a variety of cell lines. For example, IGFBP-3 has antiproliferative effects on breast cells that are unresponsive to IGF (8) and on mouse fibroblasts that lack IGF-1 receptors (9). IGFBP-3 has been shown to inhibit type-1 IGF receptor activation independently of its IGF binding affinity in breast cancer cells (25). In addition, proteolytic fragments of IGFBP-3 that have markedly reduced affinity for IGF-I retain antiproliferative effects *in vitro*. These IGFBP-3 effects may be mediated *via* cell surface binding proteins (26), nuclear binding sites (27), or other pathways (28). The IGFBP-3 NLS mutant, which is known to not translocate to the nucleus, also inhibited insulin-stimulated glucose uptake (13) Thus, it is possible that some of the insulin-antagonistic effects of IGFBP-3 are mediated *via* IGF-independent pathways that does not require nuclear localization. For example, a previously published study reports that IGFBP-3 is capable of activating a phosphotyrosine phosphatase independent of its IGF binding affinity (29). Activation of a phosphotyrosine phosphatase and subsequent de-phosphorylation could be a mechanism responsible for the decreased phosphorylated insulin receptor levels observed in our study. Of note is that Chan *et al.* (13) did not observe reduced IR phosphorylation but did see less Thr (308) phosphorylation of Akt after IGFBP-3 treatment. These investigators also did not observe an effect of IGFBP-3 on baseline (insulin-free) glucose transport, which we have. The possible differences between these studies may include either subtle differences in the experimental conditions or a different behavior of the substrain of the 3T3-L1 cells, which may be susceptible to biologic drift over time in repeat culturing as described for many other cell lines (30).

TNF-α is thought to play an important role in the pathogenesis of insulin resistance associated with obesity. In adipose tissue, levels of TNF-α and its mRNA correlate positively with the degree of obesity or hyperinsulinemia (31). TNF-α's main mechanism of action is unknown, although it has been shown to decrease insulin receptor and the insulin-receptor substrate IRS-1 phosphorylation (32) by attenuating tyrosine kinase activity and/or activating phospho-protein phosphatase-1. Here, we report that TNF-α induces the production of IGFBP-3 in 3T3-L1 adipocytes and that the insulin-antagonistic effect of TNF-α on cultured adipocytes is partially blocked by the presence of IGFBP-3 antisense. This raises the possibility that some of the insulin antagonistic activity of TNF-α may be mediated *via* induction of IGFBP-3. Such a role is not unexpected as IGFBP-3 has been shown to mediate other effects of TNF-α in various cell types (33) and has also been implicated in mediating the effects of other growth-inhibitory and apoptosis-inducing agents such as tumor suppressor gene p53 (34), retinoic acid, (35), and transforming growth factor-beta (36).

We have previously reported that IGFBP-3 is a binding partner for the ligand-dependent nuclear receptor, retinoid X receptor-α (RXR-α) and modulates its transcriptional activity (37). RXR-α is the obligate heterodimeric partner for the nuclear receptor PPAR-γ (38), which controls the transcription of genes important in the regulation of carbohydrate and lipid metabolism. TNF-α has previously been shown to antagonize PPAR-γ (39). Our observation that TNF-α appears to increase the nuclear localization of IGFBP-3 hints at the possibility that TNF-α may exert some of its insulin-antagonizing effects by modulating the transcriptional activity of PPAR-γ *via* induction and nuclear translocation of IGFBP-3.

Regardless of the possible numerous interactions of IGFBP-3 with the insulin-signaling pathway, the strength of this report is in demonstrating that IGFPB-3 rapidly induces peripheral insulin resistance in rodents, which is evident within hours. Furthermore, after several days, the degree of insulin resistance induced by IGFBP-3 is similar in magnitude to that seen in many diabetic states. This suggests that IGFBP-3 effects are important *in vivo* and may explain the alterations in insulin action during pubertal development, and in pathophysiological conditions such as in acromegaly, when IGFBP-3 levels are high.

Adiponectin, an important adipocytokine that is induced by thiazolidinediones (TZD), is closely related to insulin sensitivity (40). We also show here that IGFBP-3 inhibits adiponectin expression both at the basal state and after PPAR-γ agonist stimulation. These findings may further explain how IGFBP-3 induces insulin resistance *in vivo*.

In conclusion, our results show that IGFBP-3 is a potent inhibitor of insulin action in cultured adipocytes as well as *in vivo*. This effect is of the same magnitude as the insulin antagonistic effect of TNF-α. In addition, we show that TNF-α induces IGFBP-3 production in cultured adipocytes and that IGFBP-3 may mediate some of the insulin-antagonistic activity of TNF-α. We also show that IGFBP-3 suppresses adiponectin expression. The mechanisms of IGFBP-3-induced insulin resistance action are as yet fully uncharacterized and are likely multiple. Further studies of the role of IGFBP-3 in insulin resistance will shed light on the molecular mechanisms of insulin resistance in general and the physiologic significance of IGFBP-3 in particular.

REFERENCES

1. Baker J, Liu JP, Robertson EJ, Efstratiadis A 1993 Role of insulin-like growth factors in embryonic and postnatal growth. Cell 75:73–82
2. Moses AC, Young SC, Morrow LA, O'Brein M, Clemmons DR 1996 Recombinant human insulin-like growth factor I increases insulin sensitivity and improves glycemic control in type II diabetes. Diabetes 45:91–100
3. Guler HP, Zapf J, Froesch ER 1987 Short-term metabolic effects of recombinant human insulin-like growth factor I in healthy adults. N Engl J Med 317:137–140
4. Dohm GL, Elton CW, Raju MS, Mooney ND, DiMarchi R, Pories WJ, Flickinger EG, Atkinson SM Jr Caro JF 1990 IGF-I–stimulated glucose transport in human skeletal muscle and IGF-I resistance in obesity and NIDDM. Diabetes 39:1028–1032
5. Simpson HL, Umpleby AM, Russell-Jones DL 1998 Insulin-like growth factor-I and diabetes. Growth Horm IGF Res 8:83–95
6. Cusi K, DeFronzo R 2000 Recombinant human insulin-like growth factor I treatment for 1 week improves metabolic control in type 2 diabetes by ameliorating hepatic and muscle insulin resistance. J Clin Endocrinol Metab 85:3077–3084
7. Firth SM, Baxter RC 2002 Cellular actions of the insulin-like growth factor binding proteins. Endocr Rev 23:824–854
8. Oh Y, Gucev Z, Ng L, Muller HL, Rosenfeld RG 1995 Antiproliferative actions of insulin-like growth factors binding protein (IGFBP)-3 in human breast cancer cells. Prog Growth Factor Res 6:505–512
9. Valentinis B, Bhala A, DeAngeleis T, Baserga R, Cohen P 1995 The human insulin-like growth factor (IGF) binding protein-3 inhibits the growth of fibroblasts with a targeted disruption of the IGF-I receptor gene. Mol Endocrinol 9:361–367
10. Murphy LJ 2003 The role of the insulin-like growth factors and their binding proteins in glucose homeostasis. Exp Diabesity Res 4:213–224
11. Chan SS, Twigg SM, Firth SM, Baxter RC 2005 Insulin-like growth factor binding protein-3 (IGFBP-3) leads to insulin resistance in adipocytes. J Clin Endocrinol Metab 90:6588–6595
12. Schuller AG, Groffen C, Van Neck JW, Zwarthoff EC, Drop SL 1994 cDNA cloning and mRNA expression of the six mouse insulin-like growth factor binding proteins. Mol Cell Endocrinol 104:57–66
13. Clancy BM, Czech MP 1990 Hexose transport stimulation and membrane redistribution of glucose transporter isoforms in response to cholera toxin, dibutyryl cyclic AMP and insulin in 3T3- adipocytes. J Biol Chem 265:12434–12443
14. Ranganathan S, Davidson MB 1996 Effect of tumor necrosis factor-a on basal and insulin-stimulated glucose transport in cultured muscle and fat cells. Metabolism 45:1089–1094
15. Bradford MM 1976 A rapid and sensitive method for the quantitation of microgram quantities of protein using the principle of protein dye binding. Anal Biochem 72:248–254
16. Silha JV, Gui Y, Murphy LJ 2002 Impaired glucose homeostasis in insulin-like growth factor-binding protein-3-transgenic mice. Am J Physiol Endocrinol Metab 283:E937–E945
17. Caprio S, Amiel SA, Merkel P, Tamborlane WV 1993 Insulin-resistant syndromes in children. Horm Res 39:112–114
18. Grinspoon S, Clemmons D, Swearingen B, Klibanski A 1995 Serum insulin-like growth factor-binding protein-3 levels in the diagnosis of acromegaly. J Clin Endocrinol Metab 80:927–932
19. Alford FP, Hew FL, Christopher MC, Rantzau C 1999 Insulin sensitivity in growth hormone (GH)-deficient adults and effect of GH replacement therapy. J Endocrinol Invest 22:28–32
20. Ruan H, Lodish HF 2003 Insulin resistance in adipose tissue: direct and indirect effects of tumor necrosis factor-α. Cytokine Growth Factor Rev 14:447–455
21. Lewitt MS, Denyer GS, Cooney GJ, Baxter RC 1991 Insulin-like growth factor binding protein-1 modulates blood glucose levels. Endocrinology 129:2254–2256
22. Rajkumar K, Krsek M, Dheen ST, Murphy LJ 1996 Impaired glucose homeostasis in insulin-like growth factor binding protein-1 transgenic mice. J Clin Invest 98:1818–1825
23. Okajima T, Iwasshita M, Takeda Y, Sakamoto S, Tanabe T, Yasuda T, Rosenfeld RG 1993 Inhibitory effects of insulin-like growth factor (IGF)-binding proteins-1 and-3 on IGF-activated glucose consumption in mouse BALB/ c 3T3 fibroblasts. J Endocrinol 136:457–470
24. Yakar S, Liu JL, Fernandex AM, Wu Y, Schally AV, Frystyk J, Chernausek SD, Mejia W, LeRoith D 2001 Liver-specific IGF-I gene deletion leads to muscle insulin insensitively. Diabetes 50:1110–1118
25. Ricort JM, Binoux M 2001 Insulin-like growth factor (IGF) Binding protein-3 inhibits type 1 IGF receptor activation independently of its IGF binding affinity. Endocrinology 142:108–113
26. Oh Y, Muller HL, Phan H, Rosenfeld RG 1993 Demonstration of receptors for insulin-like growth factor binding protein-3 on Hs578T human breast cancer cells. J Biol Chem 268:26045–26048
27. Schedlich LJ, LePage SL, Firth SM, Briggs LJ, Jans DA, Baxter RC 2000 Nuclear import of insulin-like growth factor-binding protein-3 and-5 is mediated by the importin beta subunit. J Biol Chem 275:23462–23470
28. Butt AJ, Fraley KA, Firth SM, Baxter RC 2002 IGF-binding protein-3 induced growth inhibition and apoptosis do not requires cell surface binding and nuclear translocation in human breast cancer cells. Endocrinology 143:2693–2699
29. Ricort JM, Binoux M 2002 Insulin-like growth factor-binding protein-3 activates a phosphotyrosine phosphatase. Effects on the insulin-like growth factor signaling pathway. J Biol Chem 277:19448–19454
30. Welch DR, Milas L, Tomasovic SP, Nicolson GL 1983 Heterogeneous response and clonal drift of sensitivities of metastatic 13762NF mammary adenocarcinoma clones to gamma-radiation *in vitro*. Cancer Res 43:6–10
31. Saghizadeh M, Ohg JM, Garvey WT, Henry RR, Kern PA 1996 The expression of TNF by human muscle: relationship to insulin resistance. J Clin Invest 97:1111–1116
32. Hotamisligil GS, Murray DL, Choy LN, Spiegelman BM 1994 Tumor necrosis factor-a inhibits signaling from the insulin receptor. Proc Natl Acad Sci U S A 91:4854–4858
33. Rajah R, Lee KW, Cohen P 2002 Insulin-like growth factor binding protein-3 mediates tumor necrosis factor-alpha-induced apoptosis: role of Bcl-2 phosphorylation. Cell Growth Differ 13:163–171
34. Buckbinder L, Talbott R, Velasco-Miguel S, Takenaka I, Faha B, Seizinger BR, Kley N 1995 Induction of the growth inhibitor IGF binding protein 3 by p53. Nature 377:646–649
35. Gucev ZS, Oh Y, Kelley KM, Rosenfeld RG 1996 Insulin-like growth factor biding protein 3 mediates retinoic acid- and transforming growth factor B2-induced growth inhibition in human breast cancer cells. Cancer Res 56:1545–1550
36. Rajah R, Valentinis B, Cohen P 1997 Insulin-like growth factor binding protein-3 induces apoptosis and mediates the effects of transforming growth factor B1 on programmed cell death through a p53-and IGF- independent mechanism. J Biol Chem 272:12181–12188
37. Liu B, Lee HY, Weinzimer SA, Powell DR, Clifford JL, Kurie JM, Cohen P 2000 Direct functional interactions between the insulin-like growth factor-binding protein-3 and retinoid X receptor-a regulate transcriptional signaling and apoptosis. J Biol Chem 275:33607–33613
38. Mukherjee R, Davies PJ, Crombie DL, Bischoff ED, Cessario RM, Jow L, Hamann LG, Boehm MF, Mondon CE, Nadzan AM, Paterniti JR, Heyman RA 1997 Sensitization of diabetic and obese mice to insulin by retinoid X receptor agonists. Nature 386:407–410
39. Tanaka T, Itoh H, Doi K, Fukunaga Y, Hosoda K, Shintani M, Yamashita J, Chun TH, Inoue M, Masatwugu K, Sawada N, Saito T, Inoue G, Nishimura H, Yoshimasa U, Nakao K 1999 Down regulation of peroxisome proliferator-activated receptor expression by inflammatory cytokines and its reversal by thiazolidinediones. Diabetologia 42:702–710
40. Kern PA, Di Gregorio GB, Lu T, Rassouli N, Ranganathan G 2003 Adiponectin expression from human adipose tissue: relation with obesity, insulin resistance, and tumor necrosis factor-α expression. Diabetes 52:1779–1785

Oncogene (2007) 26, 1811–1819

www.nature.com/onc

ORIGINAL ARTICLE

Insulin-like growth factor-binding protein-3 inhibition of prostate cancer growth involves suppression of angiogenesis

B Liu[1], K-W Lee[1], M Anzo[1], B Zhang[2], X Zi[3], Y Tao[4], L Shiry[5], M Pollak[4], S Lin[6] and P Cohen[1]

[1]Division of Pediatric Endocrinology, Department of Pediatrics, Mattel Children's Hospital, David Geffen School of Medicine, UCLA, Los Angeles, CA, USA; [2]Center of Developmental Biology and Genetics, College of Life Sciences, Peking University, Beijing, PR China; [3]Department of Urology and Chao Family Comprehensive Cancer Center, UCI, Irvine, CA, USA; [4]Division of Experimental Medicine, Department of Medicine and Department of Oncology, McGill University, Montreal, QC, Canada; [5]INSMED Corp., Glen Allen, Charlottesville, VA, USA and [6]Department of Molecular, Cell and Developmental Biology, UCLA, Los Angeles, CA, USA

Insulin-like growth factor-binding protein-3 (IGFBP-3) is a multifunctional protein that induces apoptosis utilizing both insulin-like growth factor receptor (IGF)-dependent and -independent mechanisms. We investigated the effects of IGFBP-3 on tumor growth and angiogenesis utilizing a human CaP xenograft model in severe-combined immunodeficiency mice. A 16-day course of IGFBP-3 injections reduced tumor size and increased apoptosis and also led to a reduction in the number of vessels stained with CD31. *In vitro*, IGFBP-3 inhibited both vascular endothelial growth factor- and IGF-stimulated human umbilical vein endothelial cells vascular network formation in a matrigel assay. This action is primarily IGF independent as shown by studies utilizing the non-IGFBP-binding IGF-1 analog Long-R3. Additionally, we used a fibroblast growth factor-enriched matrigel-plug assay and chick allantoic membrane assays to show that IGFBP-3 has potent antiangiogenic actions *in vivo*. Finally, overexpression of IGFBP-3 or the non-IGF-binding GGG-IGFBP-3 mutant in Zebrafish embryos confirmed that both IGFBP-3 and the non-IGF-binding mutant inhibited vessel formation *in vivo*, indicating that the antiangiogenic effect of IGFBP-3 is an IGF-independent phenomenon. Together, these studies provide the first evidence that IGFBP-3 has direct, IGF-independent inhibitory effects on angiogenesis providing an additional mechanism by which it exerts its tumor suppressive effects and further supporting its development for clinical use in the therapy of patients with prostate cancer.
Oncogene (2007) **26**, 1811–1819. doi:10.1038/sj.onc. 1209977; published online 18 September 2006

Keywords: insulin-like growth factor-binding protein-3; prostate cancer; angiogenesis; apoptosis

Correspondence: Professor P Cohen, Division of Pediatric Endocrinology, Department of Pediatrics, Mattel Children's Hospital, David Geffen School of Medicine, UCLA, Los Angeles, CA 90095, USA.
E-mail: hassy@mednet.ucla.edu
Received 2 March 2006; revised 1 August 2006; accepted 4 August 2006; published online 18 September 2006

Introduction

Regulation of cellular growth and development by the insulin-like growth factors (IGFs) is well accepted and interventions that block the IGF axis as such are currently in development for cancer therapy (Jones *et al*., 2005). In addition, various components of this axis are modulated by dietary and pharmacological cancer interventions (Voskuil *et al*., 2005).

Insulin-like growth factor-binding protein-3 (IGFBP-3), one of six members of the IGFBP family that noncovalently bind to IGFs with high affinity, is the most abundant in human serum (for a review see Firth and Baxter, 2002). IGFBP-3 is a multifunctional protein that transports and stabilizes IGFs in circulation; modulates IGF bioactivity; inhibits the growth of cancer cells; and induces apoptosis of cancer cells. The effects of IGFBP-3 on cell growth and apoptosis involve both sequestering IGFs from their receptors and IGF-independent mechanisms that include: binding to retinoid X receptor (RXR) and modulation of nuclear signalling followed by nucleomitochondrial translocation of RXR/Nur77 and induction of rapid apoptosis (Lee *et al*., 2005); binding to membrane receptors (Huang *et al*., 2003); and antagonism of the recently described survival factor, humanin (Ikonen *et al*., 2003). We have recently reported the initial description of successful therapeutic use of IGFBP-3 as a cancer therapy *in vivo*, and demonstrated that combination treatment of IGFBP-3 and RXR ligand had a synergistic effect on apoptosis induction leading to substantial inhibition of prostate cancer xenograft growth (Liu *et al*., 2005).

We hypothesized that apart from apoptosis induction, IGFBP-3 might have direct effects on angiogenesis because: (1) IGFBP-3 contains a highly basic heparin-binding area, and specifically binds to vascular endothelial cell monolayers (Booth *et al*., 1996) in a manner that may affect vascular angiogenesis; (2) IGFBP-3 inhibits vascular endothelial growth factor (VEGF)-mediated survival of human umbilical vein endothelial cells (HUVEC) in an IGF-independent mechanism (Zadeh and Binoux, 1997; Franklin *et al*., 2003) and

may also affect angiogenesis *in vivo*; (3) IGFBP-3 is transcriptionally upregulated during hypoxia, a potent stimulator of angiogenesis (Diaz-Gonzalez *et al*., 2005) in endothelial cells (Koong *et al*., 2000); and (4) IGFBP-3 mRNA is predominantly expressed in the vascular endothelial cells of human (Fraser *et al*., 2000), rat (Erickson *et al*., 1993), and bovine corpus lutea (Brown and Braden, 2001), which suggest a possible involvement in angiogenesis regulation, perhaps as part of a feedback mechanism. Other reports also indicate that IGFBP-3 mRNA is more abundantly expressed in hypoxia-associated inflammatory angiogenesis (Tucci *et al*., 1998; Lee *et al*., 1999) and tumor endothelial cells (Schmid *et al*., 2003). Importantly, a recent publication identifies IGFBP-3 as a farnesyl transferase inhibitor-induced negative regulator of angiogenesis in head and neck squamous cell carcinoma (Oh *et al*., 2006).

Here, we report that IGFBP-3 has direct, IGF-independent inhibitory effects on angiogenesis. Solid tumors require a supply of blood vessels to survive, grow and metastasize (Folkman, 2004) and treatments that address these issues can be more effective than nonspecific chemotherapies. Our results reveal a unique mechanism by which IGFBP-3 exerts its tumor suppressive effects and supports further investigation into the clinical translation of IGFBP-3 as a neoadjuvant in prostate cancer therapy.

Results

IGFBP-3 inhibits the growth of 22RV-1 prostate cancer xenografts in vivo

To examine the effects of IGFBP-3 as a single therapy on inhibiting prostate cancer tumor cell growth *in vivo*, male severe-combined immunodeficiency (SCID) mice with 22RV-1 prostate cancer xenografts were given daily injections of saline, or IGFBP-3 (30 mg/kg/day intraperitoneally (i.p.)) for 16 days. Treatment with IGFBP-3 resulted in significant tumor size inhibition (40% growth inhibition, $P<0.005$; $n=10$) relative to control animals (Figure 1a). A greater effect (50% inhibition) was seen for IGFBP-3 therapy on tumor weight (Figure 1b). These studies show that treatment of IGFBP-3 as a single therapy inhibits the growth of 22RV1 prostate cancer xenografts.

Induction of tumor apoptosis by IGFBP-3

Inhibition of xenograft growth by IGFBP-3 and RXR ligand is associated with an increase in apoptosis and activated Caspase-3 (Liu *et al*., 2005). The effect of IGFBP-3 single therapy on apoptosis in this xenograft model was examined by light microscopic terminal nucleotidyl transferase-mediated nick end labeling (TUNEL) assay. Representative photographs are shown in Figure 2a. As shown in Figure 2b, quantification of TUNEL-positive cells was increased sevenfold in the IGFBP-3 treatment group over saline-treated tumors. We next assessed whether this effect of IGFBP-3 is associated with an *in vivo* activation of Caspase-3. Microscopic examination of tumor sections stained for Caspase-3 clearly showed an increased detection of Caspase-3 in the IGFBP-3 therapy group as compared with the control group (Figure 2c). Quantification of Caspase-3-positive staining was increased sevenfold in IGFBP-3 treatment group over saline-treated tumors (Figure 2d). To further evaluate if regulation of cellular proliferation is also involved in the actions of IGFBP-3 on prostate cancer xenografts, we stained the tumors with the proliferation marker proliferating cell nuclear antigen (PCNA), and as shown in Figure 2e, observed no difference between IGFBP-3 and saline treatment (quantified in Figure 2f), suggesting that IGFBP-3-mediated inhibition of tumor growth does not involve regulation of cell proliferation. Negative controls, in which PCNA antibodies were omitted, did not show any positive staining (data not shown). This is in agreement with our previous observation utilizing a lower dose of IGFBP-3 (Liu *et al*., 2005).

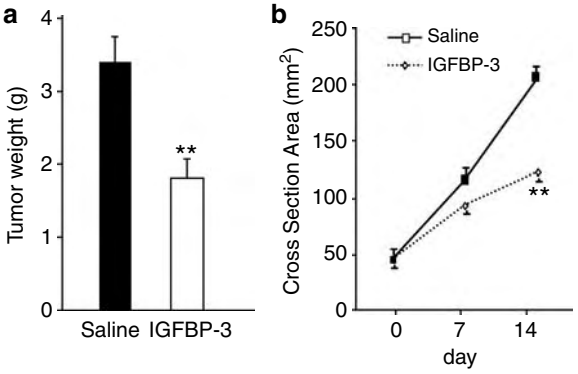

Figure 1 IGFBP-3 inhibits the growth of 22RV1 prostate cancer xenografts *in vivo*. (**a**) Tumor weights of 22RV1 CaP xenografts ($n=10$ per group) treated with or without IGFBP-3 (30 mg/kg/day), for 16 days. $^{**}P<0.005$ as compared with saline treatment. (**b**) Calculated tumor volume of 22RV1 CaP xenografts in this same experiment.

IGFBP-3 decreases vessel formation in vivo

Microvessel density, a measurement used for quantifying intratumoral angiogenesis activity, has been suggested as a valuable prognostic marker in prostate carcinoma (Weidner *et al*., 1993). To investigate if IGFBP-3 had any effect on intratumoral angiogenesis, we carried out immunohistochemical staining using an antibody against CD31, an endothelial cell-specific antigen, to evaluate the antiangiogenic effect of IGFBP-3 on 22RV1 tumor xenografts. As shown in Figure 3, a twofold increased number of CD31-positive microvessels and endothelial cells were found in the control group compared to the IGFBP-3-treated group. Our results indicate that IGFBP-3 is able to suppress prostate cancer angiogenesis through inhibiting microvessel formation.

IGFBP-3 inhibits both IGF- and VEGF-induced vascular formation

VEGF is one of the most potent angiogenic factors affecting endothelial proliferation, motility and vascular

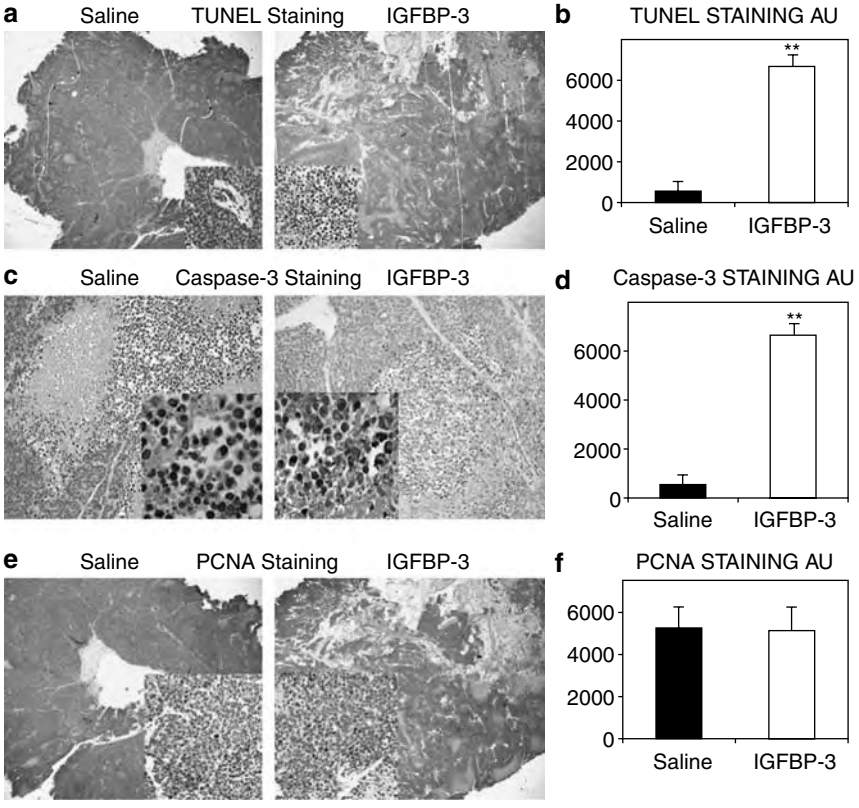

Figure 2 Inhibition of xenograft growth by IGFBP-3 is associated with an increase in apoptosis but does not involve a change in cell proliferation. (**a**) TUNEL immunohistochemistry of xenografts in control with saline treatment (left) and treatment with IGFBP-3 (right). (**b**) TUNEL pixel histogram quantitation. $^{**}P<0.005$ as compared with control ($n=10$ per group). (**c**) Microscopic examination of tumor sections stained for activated Caspase-3 antigen in control with saline treatment (left), and treatment with IGFBP-3 (right). (**d**) Quantification of Caspase-3-positive staining per pixel histogram ($n=10$ per group). (**e**) Proliferating cell nuclear antigen immunohistochemistry of xenografts in control with saline treatment (left), and treatment with IGFBP-3 (right). (**f**) Proliferating cell nuclear antigen pixel histogram quantitation ($n=10$ per group). $^{**}P<0.005$ as compared with saline control.

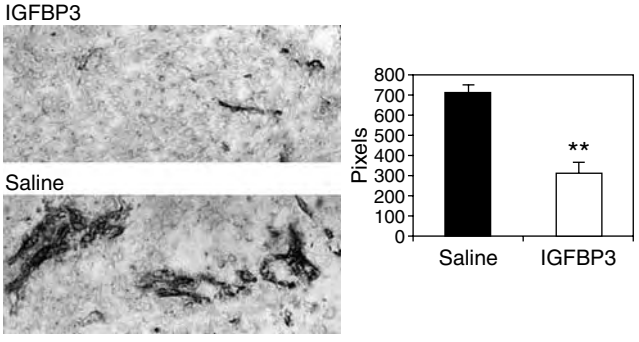

Figure 3 IGFBP-3 decreases vessel formation *in vivo*. Immunohistochemical staining of xenografts using CD31 antibody. (**a**) Control with saline treatment and IGFBP-3 treatment. (**b**) Quantification of CD31-positive staining by pixel histogram ($n=10$ per group).

permeability. VEGF binds with high affinity to the tyrosine kinase receptors *Flt-1* (VEGFR-1) and *Flk-1/KDR* (VEGFR-2) expressed by endothelial cells (Ferrara, 2001). VEGF expression by prostate cancer specimens is far greater than that by stromal cells of the normal prostate. These observations suggest that VEGF plays a role on tumor cell activation (autocrine regulation), in addition to paracrine actions, whereby it regulates endothelial cell (EC) functions and subsequent neovascular development (Jackson *et al*., 1997). We further investigated the effect of IGFBP-3 on VEGF-regulated vascular formation, using an established *in vitro* model of human endothelial cellular vessel formation in matrigel (Iwatsuki *et al*., 2005). IGFBP-3 alone has no effect on vascular formation in this assay; however, VEGF stimulated substantial new vascular complex formation. Importantly, VEGF-induced vessel formation was completely inhibited by IGFBP-3 cotreatment (Figure 4).

To further explore if effect of IGFBP-3 on VEGF-regulated vascular formation and to examine its effects on IGF-regulated vascular formation and to determine if this is an IGF-independent action, human endothelial cells on matrigel were treated individually with IGF-1, IGFBP-3, Long R3-IGF-1 (an IGF-1 analog which does not bind IGFBP-3) or their combination (Figure 4). IGF-1 stimulated vascular formation consistent with its described angiogenic effect (Hanahan and Folkman, 1996). IGFBP-3 blocked the angiogenic effect of IGF-1. Long R3-IGF-1, which does not bind IGFBP-3 also stimulates vascular formation and is partially blocked by IGFBP-3, indicating that IGFBP-3 interferes with

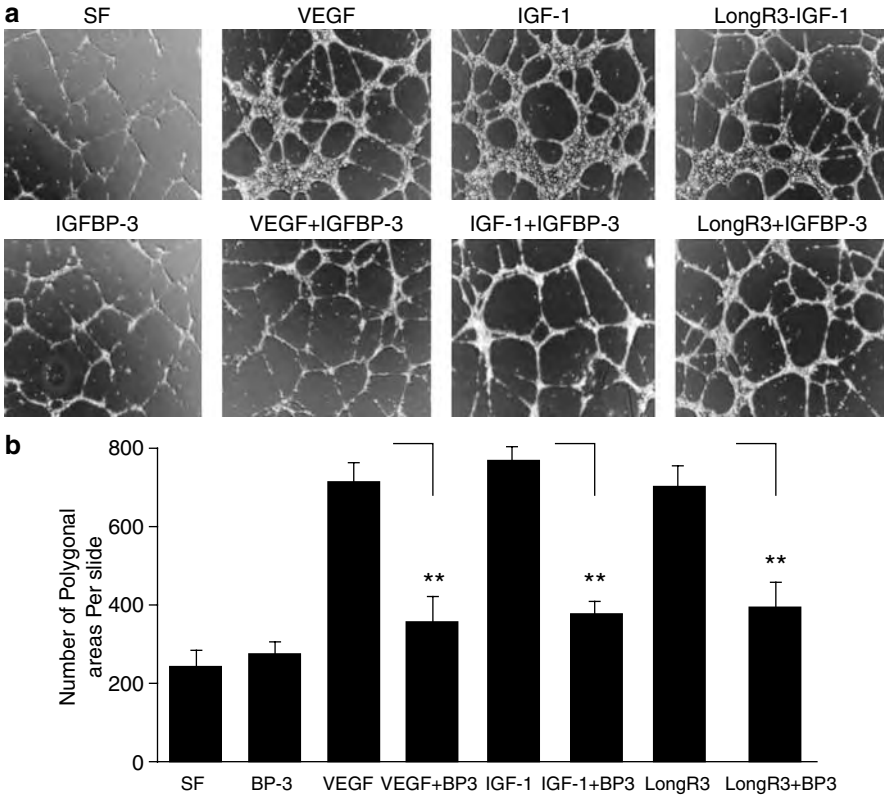

Figure 4 IGFBP-3 inhibits VEGF- and IGF-regulated vascular formation. (**a**) Representative pictures of human umbilical vein endothelial cellular vessel formation in matrigel under several treatment conditions. (**b**) Quantification of vessel formation ($n=6$ per group).

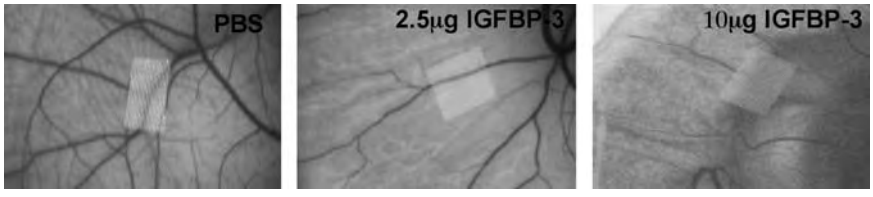

Figure 5 Antiangiogenic effects of rhIGFBP-3 on the CAM assay. Methylcellulose disks containing PBS, 2.5 and 10 μg of IGFBP-3 were implanted on CAMs of 6-day-old chick embryos. After 3–4 days, the formation of avascular zone was examined under a stereoscope. Each treatment was repeated in six chick CAMs with similar results.

IGF-induced vascular formation in part via an IGF-1-independent mechanism.

IGFBP-3 inhibits in vivo *angiogenesis*

To investigate the antiangiogenic activity in an *in vivo* setting, rhIGFBP-3 was tested on chicken embryo chick allantoic membrane (CAM) and murine matrigel plug angiogenesis assays. Compared to phosphate-buffered saline (PBS) control, IGFBP-3 at doses of 2.5 and 10 μg/disk completely inhibited the growth of new vascular vessels in all six tested chick embryos, which was measured by the formation of avascular zones (Figure 5). No inflammation was observed in these studies.

Basic fibroblast growth factor (bFGF)-induced angiogenesis has been considered as a model of tumor-derived neovacularization (Klauber *et al*., 1997). Figure 6 shows that the bFGF plugs were bright red and contained a large numbers of micro-blood vessels, which penetrated into the solidified martrigel and spread widely. There were no blood vessels in the PBS plugs (data not shown). However, the numbers of micro-blood vessels decreased in the plugs with both bFGF and different doses of rhIGFBP-3 in a dose-dependent manner. Quantification by image analysis showed that bFGF-induced neovascularizations were inhibited by 17 and 75% at the doses of 2.5 and 5 μg/ml rhIGFBP-3, respectively. Addition of 10 μg/ml of IGFBP-3 to FGF-2 was not significantly different from the 5 μg/ml dose.

Overexpression/ectopic expression of human IGFBP-3 inhibits vascular patterning in Zebrafish embryos in an IGF-independent manner

To assess the role of IGFBP-3 in blood vessel patterning *in vivo*, we overexpressed/ectopic expressed human

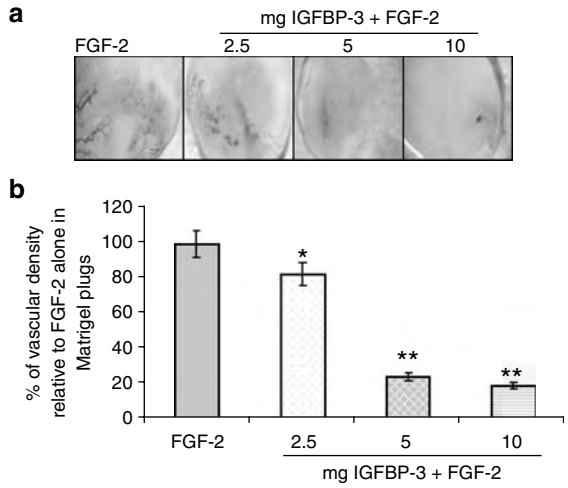

Figure 6 Antiangiogenic effects of rhIGFBP-3 on a bFGF-enriched matrigel plug. Mice received subcutaneous injection of 300 ml of a matrigel mixture containing FGF-2 with or without rhIGFBP-3. The animals were killed and dissected 2 weeks later, and the matrigel plugs were exposed and photographed. (**a**) A photograph of a representative matrigel plug from each group was shown. (**b**) Pixel histogram quantitation of percentages of vascular density in matrigels with FGF-2 and different doses of IGFBP-3 compared to FGF-2 alone was shown. Each group contained six animals. $*P<0.05$, $**P<0.01$ (FGF2 versus FGF2 + IGFBP-3, Student's *t*-test).

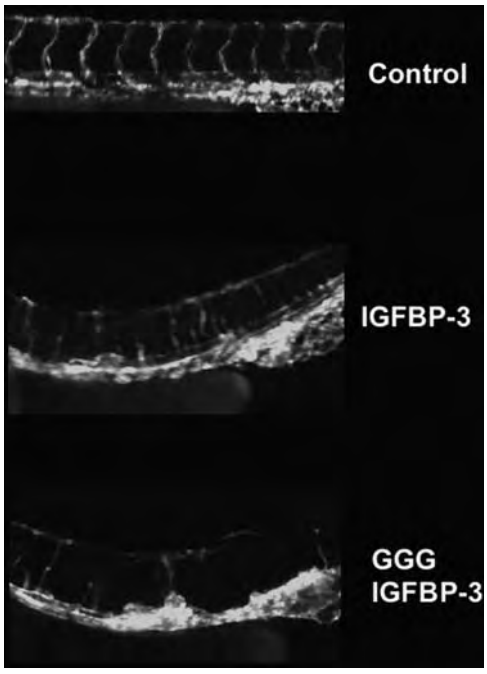

Figure 7 Overexpression/ectopic expression of human IGFBP-3 affects vascular patterning in Zebrafish embryos in an IGF-independent manner. Embryos from *flk1*:GFP transgenic Zebrafish were injected with 300 pg of capped mRNA derived by *in vitro* transcription from either wild-type or IGF-binding defective human IGFBP3 cDNA at one-cell stage and observed at 36 h.p.f. The fluorescent micrographs showing vascular patterning reflected by GFP expression in control embryos are shown as are those from embryos injected with wild-type IGFBP-3 mRNA or mutant IGFBP-3 mRNA.

IGFBP-3 via injection of the corresponding mRNA into the cytoplasm of one-cell stage flk1:green fluorescent protein (GFP) transgenic Zebrafish embryos. flk1:GFP represents a stable integration of a GFP reporter gene driven by the promoter of VEGF receptor-2 (flk1) and it utilized in the rapid, high-throughput screening of antiangiogenesis drug screening (Cross *et al*., 2003). As the vascular endothelial cells are labeled with green fluorescence, the blood vessels can be easily visualized in live embryos in this transgenic fish line. As shown in Figure 7, introduction of IGFBP-3 (300 pg of mRNA) resulted in defects of vascular patterning in the trunk and tail regions (Figure 7) in 36 h.p.f. (hours post fertilization) embryos. Intersegmental vasculogenesis is severely affected. Vessels are lacking and the remaining vessels are abnormally positioned. In addition, regional somites are compressed compared to control fish. To test whether the observed effect is dependent on the function of IGFBP-3 in IGF-sequestration, mRNA from a mutant form of IGFBP-3 which is defective in IGF binding was injected into flk1:GFP embryos in parallel with wild-type form. The phenotype in embryos injected with the mutant form is essentially indistinguishable from that with wild-type IGFBP-3, indicating that the effect of IGFBP-3 on vasculogenesis is independent of IGF sequestration. These apparently dorsalized embryos resemble previously characterized Zebrafish mutants such as the notochord mutant ntl, which shows defects in notochord differentiation (Odenthal *et al*., 1996) as well as the dominant-negative IGF-1R overexpression mutant (Eivers *et al*., 2004).

Discussion

In prostate cancer, as in other cancers, tumor-associated angiogenesis is a crucial step in the process of tumor growth, invasion and metastasis (van Moorselaar and Voest, 2002). Previous studies on prostate cancers have demonstrated a correlation between microvessel density, pathological stage and Gleason score (Arakawa *et al*., 1997; Bettencourt *et al*., 1998; Bono *et al*., 2002). Therefore, inhibiting vessel formation offers hope to reduce the morbidity and mortality from prostate cancer, and solid tumor cancers in general (Folkman, 1971).

Two reports have shown that IGFBP-3 inhibited the growth of bovine aortic endothelial cells (Delafontaine *et al*., 1996) and the IGF-/VEGF-induced proliferation of HUVEC (Franklin *et al*., 2003). In addition, IGFBP-3 is inhibitory for both proliferation and *in vitro* angiogenesis of the mouse endothelial progenitor cell line AEL-R1/LRT-*Runx1* in a manner independent from growth inhibitory effects of IGFBP-3 (Iwatsuki *et al*., 2005). This was shown to be specific to IGFBP-3 as IGFBP-6 was not inhibitory for *in vitro* angiogenesis of AEL-R1/LRT-*Runx1* cells, even at a higher concentration.

It has been reported that VEGF and transforming growth factor 1 downregulate the expression

of *IGFBP-3* in aortic endothelial cells (Erondu *et al*., 1996; Dahlfors and Arnqvist, 2000), whereas IGF, tumor necrosis factor-α and interleukin-1 upregulate it in endothelial cells or articular chondrocytes (Olney *et al*., 1995; Erondu *et al*., 1996). Thus, *IGFBP-3* may be a downstream effector for many growth regulatory cytokines and its transcription must be regulated differently depending on the cell type. Indeed, knockdown of IGFBP-3 expression by RNA interference or neutralizing antibodies blocked the antiangiogenic effect of the farnesyl transferase inhibitor SCH66336 in head and neck squamous cell carcinoma (Oh *et al*., 2006).

IGFBP-3 is known to be overexpressed during the angiogenic phase of the corpus luteum in rats, primates and humans (Erickson *et al*., 1993; Fraser *et al*., 1998, 2000). Other reports also indicate that IGFBP-3 mRNA is more abundantly expressed in hypoxia-associated inflammatory angiogenesis (Tucci *et al*., 1998; Lee *et al*., 1999) and tumor endothelial cells (Schmid *et al*., 2003). Indeed, hypoxia is the major pathophysiological condition regulating angiogenesis, and increased angiogenesis in response to hypoxia is part of an adaptive response aimed at achieving increased delivery of oxygen and nutrients to tissues (Acker and Plate, 2003). IGFBP-3 is induced by hypoxia (Grimberg *et al*., 2005) and may be involved in the normalization of tumor vasculature, modulating the abnormal structure and function of tumor vasculature (Jain, 2005).

Chan *et al*. (1998) demonstrated that plasma level of IGFBP-3 was a predictor of advanced-stage prostate cancer (relative risk = 0.2, 95% confidence interval 0.1–0.6 for the highest versus the lowest quartiles of IGFBP-3). Lee *et al*. (2002) has reported that the overexpression of rhIGFBP-3 by an adenoviral vector, Ad5CMV, inhibited the growth of non-small-cell lung cancer cells in tumor xenografts. Singh *et al*. (2004b) showed that the antitumor effects of both grape seed extract and inositol hexaphosphate (Singh *et al*., 2004a) were associated with a concomitant rise in serum IGFBP-3 and importantly, suppression of angiogenesis as measured by tumor vessel immunohistochemistry and serum VEGF levels. Silibinin, an antioxidant flavonoid, also inhibits prostate cancer xenograft growth and was associated with a decrease in tumor VEGF staining as well as increased intracellular IGFBP-3 staining (Singh *et al*., 2003) in mice.

Evidence for IGF-independent actions of IGFBP-3 include: (1) effects on cells that lack a functional type 1 IGF receptor (Valentinis *et al*., 1995); (2) IGFBP-3 binds other protein partners (receptors) that are not associated with IGFs (Liu *et al*., 2000; Huang *et al*., 2003; Ikonen *et al*., 2003); and as supported in the current study, (3) IGF analogs that do not bind IGFBP-3 fail to block IGFBP action (Franklin *et al*., 2003); and (4) IGFBP-3 mutants that do not bind IGFs maintain biologic actions (Chan *et al*., 2005). In the present study, we further support this concept by demonstrating antagonism of VEGF action and reporting data utilizing a mutant form of IGFBP-3 with greatly reduced IGF binding in Zebrafish.

In summary, these data provide evidence for the first time that rhIGFBP-3 has direct inhibitory effects on angiogenesis. As invasion and angiogenesis are important determinants of tumor progression, this newly described function of IGFBP-3 could have important relevance to both the prediction of cancer progression as a biomarker and cancer therapy as a therapeutic target. Collectively, these results suggest that inhibition of human prostate cancer growth by IGFBP-3 is associated with its *in vivo* antiproliferative, proapoptotic and antiangiogenic efficacy and supports further research into the potential clinical use of IGFBP-3 or pharmacological inducers of IGFBP-3 as neoadjuvant approaches for patients with prostate cancer.

Materials and methods

Cell culture

22RV1 cells were from ATCC (Manassas, VA, USA) and maintained as directed. HUVEC and Microvascular Endothelial Cell Growth Medium Bullet Kit-2 (EGM-2-MV Bullet Kit) were purchased from Clonetics (San Diego, CA, USA) and maintained as directed. All cultures were incubated at 37°C in a humidified atmosphere containing 5% CO_2.

Tumor xenografts

22RV1 xenograft tumors were generated by injection of 1×10^6 cells in 200 μl mixed at a 1:1 dilution with matrigel in the right flank of male SCID mice. Tumors were established for 2 weeks before the start of treatment. Ten SCID mice with 22RV1 tumors were treated daily with saline or IGFBP-3 (30 mg/kg/day), given by daily i.p. injections for 16 days. The length and width of the mass located at the site of injection of the 22RV1 cells were measured with calipers and recorded once a week. The mice were killed at day 16. Tumors were harvested, weighed, fixed in formaldehyde and embedded in paraffin. Animal care was in accordance with current regulations and standards of the National Institutes of Health, as well as our institutional guidelines for animal care. All animal experiments were approved by the animal research committee of the institutional review board.

Tumor immunohistochemistry

Paraffin-embedded sections were prepared from 22RV1 tumors harvested on day 16. After deparaffinization of tissue section, apoptotic DNA fragments were labeled by terminal deoxynucleotidyl transferase, and detected by antidigoxigenin antibody conjugated to fluorescein (ApopTag fluorescein *in situ* apoptosis detection kit, Chemicon, Temecula, CA, USA). Cells were examined at $\times 40$ using an inverted fluorescence microscope (Axiovert 135M, Carl Zeiss, New York, NY, USA). Apoptotic staining was quantified by pixel histogram (Adobe Systems, Mountain View, CA, USA) and confirmed by manual counting ($r = 0.98$) by counting the positive cells (brown-stained), as well as the total number of cells in 10 arbitrarily selected fields by an independent observer. Indirect immunohistochemistry was performed with Vectastain Elite ABC kit (Vector Labs, Burlingame, CA, USA) using 3,3′-diaminobenzidine as a chromogen and quantitated as per TUNEL assay above. Sections were incubated with mouse monoclonal antibodies against PCNA (Ab-1, 1:2500; Oncogene Science, Manhasset, NY, USA), CD31 (JC70A, 1:20; Dako Corp., Carpinteria, CA, USA),

activated Caspase-3 antibody (Sigma, St Louis, MO, USA) overnight at 4°C in a humidified chamber. Negative controls were treated with only Tris-buffered saline under the same conditions.

In vitro *vascular formation matrigel assays*
HUVEC cells (1.5×10^5) were resuspended in 1 ml of StemPro-34 SFM complete medium (Invitrogen, Carlsbad, CA, USA) with or without recombinant human IGFBP-3 or VEGF (Sigma, St Louis, MO, USA) and overlayed on a Biocoat matrigel basement membrane (BD Biosciences, San Jose, CA, USA) in a six-well plate. After a 12–14 h incubation at 37°C, the number of polygonal areas formed by vascular tube-like structures was counted under a microscope for each well (Iwatsuki *et al*., 2005).

Materials
Recombinant human IGFBP-3 and IGF-1 were obtained from INSMED Corp. (Glen Allen, VA, USA), aliquoted and stored at −80°C. The activity of rhIGFBP-3 for both IGF-I-binding and -inhibitory effect on cell proliferation of human breast cancer MCF7 cells was confirmed by Western ligand blotting and 3-(4,5-dimethylthiazol-2-yl)-2,5-diphenyltetrazolium bromide assay as described previously (Pratt and Pollak, 1994), respectively, before the experiments (data not shown). bFGF and the rabbit antiserum against human IGFBP-3 were purchased from Upstate Inc. (Lake Placid, NY, USA). Long R3-IGF-1 was obtained from Gropep (Adelaide, Australia). Matrigel (11.46 mg/ml) was from Becton Dickinson Labware (Bedford, MA, USA).

Chicken embryo chorioallantoic membrane assay
Three-day-old fertilized white Leghorn eggs were cracked, and chicken embryos with intact yolks were carefully placed in 20×100 mm plastic Petri dishes. After 6 days of incubation in 3% CO_2 at 37°C, a disk of methylcellulose containing 10, 5 and 2.5 μg of rhIGFBP-3 dried on a nylon mesh (3×3 mm) was implanted on the CAM of individual embryos. The nylon mesh disks were made by desiccation of 10 ml of 0.45% methylcellulose in water. After 3–4 days of incubation, embryos and CAMs were examined for the formation of new blood vessels in the field of the implanted disks by a dissecting microscope. Disks of methylcellulose containing PBS were used as negative controls (Cao *et al*., 1998).

Murine matrigel plug angiogenesis assay
Angiogenesis was assayed as the growth of blood vessels from subcutaneous tissue of mice into a solid gel of reconstituted basement membranes containing the test sample. Matrigel in liquid form at 4°C was mixed with bFGF (1 μg) and with PBS, or 2.5, or 5 or 10 μg/ml rhIGFBP-3, and then injected into the abdominal subcutaneous tissue of six mice/group. At body temperature, the matrigel rapidly solidifies. Mice were killed 2 weeks later, and the matrigel plugs were exposed for photography (Bagheri-Yarmand *et al*., 1999).

Zebrafish mRNA microinjection
Templates for transcription were prepared by linearizing plasmids pcDNA3IGFBP3 (wild-type IGFBP-3) and pcDNA1GGGBP-3 (non-IGF-binding GGG mutant of IGFBP-3 (Buckway *et al*., 2001)) with *Sma*I. Capped mRNA was synthesized *in vitro* using the mMESSAGE mMACHINE Kit (Ambion, Austin, TX, USA). After purification as recommended by the manufacturer, RNA was dissolved in nuclease-free water at a concentration of approximately 500 ng/μl. The RNA was diluted to a final concentration of 100 ng/μl and injected into the cytoplasm of one-cell stage *flk1*:GFP Zebrafish embryos.

Fluorescence microscopy
Embryos were examined under a fluorescein isothiocyanate filter on a Zess microscopy (Zeiss Axioplan-2, Thornwood, NY, USA). Pictures represent an area of 500×500 μm imaged with a ×20/0.7 NA HC PlanApo lens. GFP was detected at a spectral range from 507 to 550 nm.

Statistical analysis
All *in vitro* experiments were repeated at least three times. Means ± s.d. are shown. Statistical analyses were performed using analysis of variance tests using InStat (GraphPad, San Diego, CA, USA). Differences were considered statistically significant when $^*P < 0.05$ and when $^{**}P < 0.005$.

Acknowledgements

This work was supported in part by a Prostate Cancer Foundation award and National Institutes of Health Grants RO1AG20954, P50CA92131 and RO1CA100938 (to PC), grants from the Stein-Oppenheimer Foundation, the Lawson Wilkins Pediatric Endocrinology Society, the UCLA Prostate Cancer SPORE and National Institutes of Health Grant 2K12HD34610 (to K-WL); and a National Institutes of Health Grant R01DK054508 (to SL).

References

Acker T, Plate KH. (2003). Role of hypoxia in tumor angiogenesis – molecular and cellular angiogenic crosstalk. *Cell Tissue Res* **314**: 145–155.

Arakawa A, Soh S, Chakraborty S, Scardino PT, Wheeler TM. (1997). Prognostic significance of angiogenesis in clinically localized prostate cancer (staining for factor VIII-related antigen and CD34 antigen). *Prostate Cancer Prostatic Dis* **1**: 32–38.

Bagheri-Yarmand R, Kourbali Y, Rath AM, Vassy R, Martin A, Jozefonvicz J *et al*. (1999). Carboxymethyl benzylamide dextran blocks angiogenesis of MDA-MB435 breast carcinoma xenografted in fat pad and its lung metastases in nude mice. *Cancer Res* **59**: 507–510.

Bettencourt MC, Bauer JJ, Sesterhenn IA, Connelly RR, Moul JW. (1998). CD34 immunohistochemical assessment of angiogenesis as a prognostic marker for prostate cancer recurrence after radical prostatectomy. *J Urol* **160**: 459–465.

Bono AV, Celato N, Cova V, Salvadore M, Chinetti S, Novario R. (2002). Microvessel density in prostate carcinoma. *Prostate Cancer Prostatic Dis* **5**: 123–127.

Booth BA, Boes M, Dake BL, Linhardt RJ, Caldwell EE, Weiler JM *et al*. (1996). Structure–function relationships in the heparin-binding C-terminal region of insulin-like growth factor binding protein-3. *Growth Regul* **6**: 206–213.

Brown AT, Braden TD. (2001). Expression of insulin-like growth factor binding protein (IGFBP-3), and the effects of IGFBP-2 and -3 in the bovine corpus luteum. *Domest Anim Endocrinol* **20**: 203–216.

Buckway CK, Wilson EM, Ahlsen M, Bang P, Oh Y, Rosenfeld RG. (2001). Mutation of three critical amino

acids of the N-terminal domain of IGF- binding protein-3 essential for high affinity IGF binding. *J Clin Endocrinol Metab* **86**: 4943–4950.

Cao Y, Linden P, Farnebo J, Cao R, Eriksson A, Kumar V *et al*. (1998). Vascular endothelial growth factor C induces angiogenesis *in vivo*. *Proc Natl Acad Sci USA* **95**: 14389–14394.

Chan JM, Stampfer MJ, Giovannucci E, Gann PH, Ma J, Wilkinson P *et al*. (1998). Plasma insulin-like growth factor-I and prostate cancer risk: a prospective study. *Science* **279**: 563–566.

Chan SS, Twigg SM, Firth SM, Baxter RC. (2005). Insulin-like growth factor binding protein-3 leads to insulin resistance in adipocytes. *J Clin Endocrinol Metab* **90**: 6588–6595.

Cross LM, Cook MA, Lin S, Chen JN, Rubinstein AL. (2003). Rapid analysis of angiogenesis drugs in a live fluorescent zebrafish assay. *Arterioscler Thromb Vasc Biol* **23**: 911–912.

Dahlfors G, Arnqvist HJ. (2000). Vascular endothelial growth factor and transforming growth factor-beta1 regulate the expression of insulin-like growth factor-binding protein-3, -4, and -5 in large vessel endothelial cells. *Endocrinology* **141**: 2062–2067.

Delafontaine P, Ku L, Anwar A, Hayzer DJ. (1996). Insulin-like growth factor 1 binding protein 3 synthesis by aortic endothelial cells is a function of cell density. *Biochem Biophys Res Commun* **222**: 478–482.

Diaz-Gonzalez JA, Russell J, Rouzaut A, Gil-Bazo I, Montuenga L. (2005). Targeting hypoxia and angiogenesis through HIF-1alpha inhibition. *Cancer Biol Ther* **4**: 1055–1062.

Eivers E, McCarthy K, Glynn C, Nolan CM, Byrnes L. (2004). Insulin-like growth factor (IGF) signalling is required for early dorso-anterior development of the zebrafish embryo. *Int J Dev Biol* **48**: 1131–1140.

Erickson GF, Nakatani A, Ling N, Shimasaki S. (1993). Insulin-like growth factor binding protein-3 gene expression is restricted to involuting corpora lutea in rat ovaries. *Endocrinology* **133**: 1147–1157.

Erondu NE, Dake BL, Moser DR, Lin M, Boes M, Bar RS. (1996). Regulation of endothelial IGFBP-3 synthesis and secretion by IGF-I and TGF-beta. *Growth Regul* **6**: 1–9.

Ferrara N. (2001). Role of vascular endothelial growth factor in regulation of physiological angiogenesis. *Am J Physiol Cell Physiol* **280**: C1358–66.

Firth SM, Baxter RC. (2002). Cellular actions of the insulin-like growth factor binding proteins. *Endocr Rev* **23**: 824–854.

Folkman J. (1971). Tumor angiogenesis: therapeutic implications. *N Engl J Med* **285**: 1182–1186.

Folkman J. (2004). Endogenous angiogenesis inhibitors. *Apmis* **112**: 496–507.

Franklin SF, Ferry RJ, Cohen P. (2003). Rapid insulin-like growth factor (IGF)-independent effects of IGF binding protein-3 on endothelial cell survival. *J Clin Endocrinol Metab* **88**: 900–907.

Fraser HM, Lunn SF, Kim H, Duncan WC, Rodger FE, Illingworth PJ *et al*. (2000). Changes in insulin-like growth factor-binding protein-3 messenger ribonucleic acid in endothelial cells of the human corpus luteum: a possible role in luteal development and rescue. *J Clin Endocrinol Metab* **85**: 1672–1677.

Fraser HM, Lunn SF, Kim H, Erickson GF. (1998). Insulin-like growth factor binding protein-3 mRNA expression in endothelial cells of the primate corpus luteum. *Hum Reprod* **13**: 2180–2185.

Grimberg A, Coleman CM, Burns TF, Himelstein BP, Koch CJ, Cohen P *et al*. (2005). p53-Dependent and p53-independent induction of insulin-like growth factor binding protein-3 by deoxyribonucleic acid damage and hypoxia. *J Clin Endocrinol Metab* **90**: 3568–3574.

Hanahan D, Folkman J. (1996). Patterns and emerging mechanisms of the angiogenic switch during tumorigenesis. *Cell* **86**: 353–364.

Huang SS, Ling TY, Tseng WF, Huang YH, Tang FM, Leal SM *et al*. (2003). Cellular growth inhibition by IGFBP-3 and TGF-beta1 requires LRP-1. *FASEB J* **17**: 2068–2081.

Ikonen M, Liu B, Hashimoto Y, Ma L, Lee K-W, Niikura T *et al*. (2003). Interaction between the Alzheimer's survival peptide humanin and insulin-like growth factor-binding protein 3 regulates cell survival and apoptosis. *Proc Natl Acad Sci USA* **100**: 13042–13047.

Iwatsuki K, Tanaka K, Kaneko T, Kazama R, Okamoto S, Nakayama Y *et al*. (2005). Runx1 promotes angiogenesis by downregulation of insulin-like growth factor-binding protein-3. *Oncogene* **24**: 1129–1137.

Jackson MW, Bentel JM, Tilley WD. (1997). Vascular endothelial growth factor (VEGF) expression in prostate cancer and benign prostatic hyperplasia. *J Urol* **157**: 2323–2328.

Jain RK. (2005). Normalization of tumor vasculature: an emerging concept in antiangiogenic therapy. *Science* **307**: 58–62.

Jones HE, Gee JM, Taylor KM, Barrow D, Williams HD, Rubini M *et al*. (2005). Development of strategies for the use of anti-growth factor treatments. *Endocr Relat Cancer* **12**(Suppl 1): S173–S182.

Klauber N, Parangi S, Flynn E, Hamel E, D'Amato RJ. (1997). Inhibition of angiogenesis and breast cancer in mice by the microtubule inhibitors 2-methoxyestradiol and taxol. *Cancer Res* **57**: 81–86.

Koong AC, Denko NC, Hudson KM, Schindler C, Swiersz L, Koch C *et al*. (2000). Candidate genes for the hypoxic tumor phenotype. *Cancer Res* **60**: 883–887.

Lee HY, Chun KH, Liu B, Wiehle SA, Cristiano RJ, Hong WK *et al*. (2002). Insulin-like growth factor binding protein-3 inhibits the growth of non-small cell lung cancer. *Cancer Res* **62**: 3530–3537.

Lee KW, Ma L, Yan X, Liu B, Zhang XK, Cohen P. (2005). Rapid apoptosis induction by IGFBP-3 involves an insulin-like growth factor-independent nucleomitochondrial translocation of RXRalpha/Nur77. *J Biol Chem* **280**: 16942–16948.

Lee WH, Wang GM, Yang XL, Seaman LB, Vannucci SI. (1999). Perinatal hypoxia-ischemia decreased neuronal but increased cerebral vascular endothelial IGFBP3 expression. *Endocrine* **11**: 181–188.

Liu B, Lee HY, Weinzimer SA, Powell DR, Clifford JL, Kurie JM *et al*. (2000). Direct functional interactions between insulin-like growth factor-binding protein-3 and retinoid X receptor-alpha regulate transcriptional signaling and apoptosis. *J Biol Chem* **275**: 33607–33613.

Liu B, Lee KW, Li H, Ma L, Lin GL, Chandraratna RA *et al*. (2005). Combination therapy of insulin-like growth factor binding protein-3 and retinoid X receptor ligands synergize on prostate cancer cell apoptosis *in vitro* and *in vivo*. *Clin Cancer Res* **11**: 4851–4856.

Odenthal J, Haffter P, Vogelsang E, Brand M, van Eeden FJ, Furutani-Seiki M *et al*. (1996). Mutations affecting the formation of the notochord in the zebrafish, *Danio rerio*. *Development* **123**: 103–115.

Oh SH, Kim WY, Kim JH, Younes MN, El-Naggar AK, Myers JN *et al*. (2006). Identification of insulin-like growth factor binding protein-3 as a farnesyl transferase inhibitor

SCH66336-induced negative regulator of angiogenesis in head and neck squamous cell carcinoma. *Clin Cancer Res* **12**: 653–661.

Olney RC, Wilson DM, Mohtai M, Fielder PJ, Smith RL. (1995). Interleukin-1 and tumor necrosis factor-alpha increase insulin-like growth factor-binding protein-3 (IGFBP-3) production and IGFBP-3 protease activity in human articular chondrocytes. *J Endocrinol* **146**: 279–286.

Pratt SE, Pollak MN. (1994). Insulin-like growth factor binding protein 3 (IGF-BP3) inhibits estrogen-stimulated breast cancer cell proliferation. *Biochem Biophys Res Commun* **198**: 292–297.

Schmid MC, Bisoffi M, Wetterwald A, Gautschi E, Thalmann GN, Mitola S *et al*. (2003). Insulin-like growth factor binding protein-3 is overexpressed in endothelial cells of mouse breast tumor vessels. *Int J Cancer* **103**: 577–586.

Singh RP, Sharma G, Dhanalakshmi S, Agarwal C, Agarwal R. (2003). Suppression of advanced human prostate tumor growth in athymic mice by silibinin feeding is associated with reduced cell proliferation, increased apoptosis, and inhibition of angiogenesis. *Cancer Epidemiol Biomarkers Prev* **12**: 933–939.

Singh RP, Sharma G, Mallikarjuna GU, Dhanalakshmi S, Agarwal C, Agarwal R. (2004a). *In vivo* suppression of hormone-refractory prostate cancer growth by inositol hexaphosphate: induction of insulin-like growth factor binding protein-3 and inhibition of vascular endothelial growth factor. *Clin Cancer Res* **10**: 244–250.

Singh RP, Tyagi AK, Dhanalakshmi S, Agarwal R, Agarwal C. (2004b). Grape seed extract inhibits advanced human prostate tumor growth and angiogenesis and upregulates insulin-like growth factor binding protein-3. *Int J Cancer* **108**: 733–740.

Tucci M, Nygard K, Tanswell BV, Farber HW, Hill DJ, Han VK. (1998). Modulation of insulin-like growth factor (IGF) and IGF binding protein biosynthesis by hypoxia in cultured vascular endothelial cells. *J Endocrinol* **157**: 13–24.

Valentinis B, Bhala A, DeAngelis T, Baserga R, Cohen P. (1995). The human insulin-like growth factor (IGF) binding protein-3 inhibits the growth of fibroblasts with a targeted disruption of the IGF-I receptor gene. *Mol Endocrinol* **9**: 361–367.

van Moorselaar RJ, Voest EE. (2002). Angiogenesis in prostate cancer: its role in disease progression and possible therapeutic approaches. *Mol Cell Endocrinol* **197**: 239–250.

Voskuil DW, Vrieling A, van't Veer LJ, Kampman E, Rookus MA. (2005). The insulin-like growth factor system in cancer prevention: potential of dietary intervention strategies. *Cancer Epidemiol Biomarkers Prev* **14**: 195–203.

Weidner N, Carroll PR, Flax J, Blumenfeld W, Folkman J. (1993). Tumor angiogenesis correlates with metastasis in invasive prostate carcinoma. *Am J Pathol* **143**: 401–409.

Zadeh SM, Binoux M. (1997). The 16-kDa proteolytic fragment of insulin-like growth factor (IGF) binding protein-3 inhibits the mitogenic action of fibroblast growth factor on mouse fibroblasts with a targeted disruption of the type 1 IGF receptor gene. *Endocrinology* **138**: 3069–3072.